

An LP-based, Strongly Polynomial 2-Approximation Algorithm for Sparse Wasserstein Barycenters

Steffen Borgwardt

steffen.borgwardt@ucdenver.edu University of Colorado Denver

Abstract. Wasserstein barycenters correspond to optimal solutions of transportation problems for several marginals. In many applications, data is given as a set of probability measures with finite support. The *discrete barycenters* in this setting then also are measures with finite support and exhibit favorable properties: there always exists one with a provably sparse support, and each barycenter allows a non-mass splitting optimal transport to each of the marginals. Both sparsity and non-mass split are crucial to many applications.

It is open whether the computation of a discrete barycenter is possible in polynomial time. It is possible to find an exact barycenter through linear programming, but the sizes of these programs may scale exponentially. In this paper, we prove that there is a strongly polynomial 2-approximation algorithm based on linear programming. First, we show that an exact computation over the union of supports of the input measures gives a tight 2-approximation of a barycenter. This computation can be done through a linear program that can be set up and solved in strongly polynomial time. The resulting measure is sparse, but an optimal transport may split mass. We then devise another strongly polynomial algorithm to improve this measure to one with a non-mass splitting transport of lower cost. The key aspect of this second algorithm is an update of the possible support set to resolve mass split.

Finally, we present an iterative scheme that alternates between these two algorithms. The algorithm terminates with a 2-approximation that has both a sparse support and an associated non-mass splitting optimal transport. We conclude with some sample computations and an analysis of the scaling of our algorithms, exhibiting vast improvements in running time over exact LP-based computations and lower practical errors than the guaranteed 2-bound.

Keywords: discrete barycenter, optimal transport, 2-approximation, linear programming

MSC: 90B80, 90C05, 90C46, 90C90

1 Introduction

Transportation problems for several marginals arise in applications ranging from finance and economics [4,24,39,37] to physics [11,17], to economics [13,15], statistics [7,8,33], and data analytics [20,23]. The so-called *Wasserstein barycenters* correspond to optimal solutions to these problems, and have seen much recent attention. Barycenters are intimately connected to Fréchet means in Euclidean space [35,45,46,51], which is one of the origins of this field of research and the reason why statistical and probability notation is commonly used.

Given probability measures P_1, \dots, P_N on \mathbb{R}^d and a weight vector $\lambda = (\lambda_1, \dots, \lambda_N) \in \mathbb{R}_{>0}^N$ with $\sum_{i=1}^N \lambda_i = 1$, a (λ -weighted) Wasserstein barycenter is a probability measure \bar{P} on \mathbb{R}^d which satisfies

$$\phi(\bar{P}) := \sum_{i=1}^N \lambda_i W_2(\bar{P}, P_i)^2 = \inf_{P \in \mathcal{P}^2(\mathbb{R}^d)} \sum_{i=1}^N \lambda_i W_2(P, P_i)^2, \quad (1)$$

where W_2 is the quadratic Wasserstein distance and $\mathcal{P}^2(\mathbb{R}^d)$ is the set of all probability measures on \mathbb{R}^d (with finite second moments). We recommend the monographs [47,48], and the more recent [36,38], for a review of the Wasserstein distance and an overview of the literature on optimal transport problems.

1.1 Exact, approximate and heuristic algorithms

Exact barycenter computations are intractable outside of some special cases, in particular because an evaluation of the Wasserstein distance itself is already challenging. Because of this, the literature uses several types of simplifications to facilitate practical computations. One of the most important ones is to work with discrete data:

In many applications, data is given as a set of *discrete probability measures* P_1, \dots, P_N having finite support in \mathbb{R}^d . A *discrete Wasserstein barycenter* is a probability measure \bar{P} which satisfies Eq. (1) for such measures. Discrete probability measures arise naturally in many applications in operations research. The finite support corresponds to a set of geographical locations (customers, facilities, service providers) and the measures represent data that varies over time. In computer graphics or image science, discrete probability measures are supported on a grid or arise through a discretization of the underlying space.

In [2], some theoretical results were developed for these discrete barycenters. They mirror the continuous case, established in [1], with a few notable exceptions. First, unlike in the continuous case, there may exist several discrete barycenters for the same set of measures. All of them have finite support and there always exists a discrete barycenter with provably sparse support. Analogously to the continuous case, a discrete barycenter always has a non-mass splitting optimal transport to each discrete marginal, i.e., each barycenter support point transports its whole mass to just a single support point for each measure. These results were proven for uniform $\lambda_i = \frac{1}{n}$ in [2], but are readily transferred to general λ_i ; see [34]. Both sparsity and non-mass split are crucial to applications: Sparsity is desirable in many applications of operations research such as facility location. Non-mass split is often imposed by physical limitations of applications, such as the design of deformable templates [8,25,45]. For example, in metal shaping, sheets of metal have to be pressed into a collection of different shapes. Each of these shapes is modeled as a measure. A ‘mean deformation’ (barycenter) is a best shape for the initial sheet of metal with respect to the energy required to mold (transport) it into all required shapes. Only because of the existence of a non-mass splitting transport, the mean deformation can indeed be transformed into each shape through only bending and stretching. See [8] for more details on these applications.

We are interested in the computation of a discrete barycenter that exhibits these beneficial properties. It is open whether the computation of an exact discrete barycenter can be done in polynomial time. It is well-known that linear programming can be used to approximate or solve optimal transport problems [42,50]. Most importantly, exact discrete barycenters can be computed by linear programming [2,10,14]. However, these programs may scale exponentially in the number of measures N (see Section 2) and thus have not been widely considered for practical use. Much larger and faster practical computations are possible through various heuristics that fundamentally differ from LP-based approaches. Most of these algorithms are based on simplifications to the Wasserstein distance to obtain an easier objective function.

The arguably most popular tools are entropic regularization techniques, which are used to make the objective function smooth and strictly convex [18]. In recent years there has been significant progress on these techniques and they led to a flurry of competitive algorithms for good approximations of barycenters in practice. For example, regularization is used in a well-behaved implementation of a gradient descent algorithm that uses information from both smoothed primal and dual optimal transport formulations [19]. Further, regularization not only greatly simplifies the underlying optimal transport problem itself, but the regularized barycenter problem then also allows the efficient computation of iterative Bregman projections [5]. Iterative Bregman methods have proven to be a state-of-the-art solution ap-

proach for large-scale computations [49,50]; their number of variables scales roughly linearly in the number of marginals. The entropy regularized Wasserstein distance converges towards the actual Wasserstein distance in $O(\frac{1}{w})$, where w is the entropic regularization factor, and the non-regularized transport cost computed with an entropy regularized transport plan converges towards the Wasserstein distance in $O(e^{-w})$ [5,12,30]. The factor w is typically chosen through cross-validation.

The great scalability of regularization-based methods, see for example [40], comes at the cost of a few drawbacks: First, they typically require a fixed support over which a barycenter approximation is to be computed. For grid-structured data, approaches in the literature usually just pass the underlying grid as the support set. One of the results in this paper is that doing so, by itself, leads to an approximation error of up to 2 - an exact optimum over the original support is only a (possibly tight) 2-approximation of an exact barycenter, which is contained not in the original grid, but in an N -times finer grid. An additional challenge lies in scenarios where measures with sparse support are spread out over a large region, or where they lie in high dimension, such that it is not feasible to discretize the whole underlying space. These restrictions have led to interest in (different) approaches where the support for a barycenter approximation [16,22,31] or a discretization of the input measures [43] is not part of the input. Second, regularization leads to fully dense solutions, which are considered an undesirable ‘blur’ in many applications. This contrasts with the search for sparse exact or approximate barycenters like in this paper. Post-processing could be used to ‘sparsify’ a dense solution, but, to the author’s best knowledge, it has not been studied yet whether this can be done in a way to retain a provable approximation guarantee or to obtain a non-mass splitting transport. And third, they sometimes exhibit poor numerical behavior as regularization decreases [26]; often a fixed number of iterations is hard-coded.

There are other successful algorithms that do not rely on smoothing or regularization: For example, a non-smooth optimization algorithm based on quasi-Newton steps and the fast computation of super-gradients finds results that are close to an exact barycenter in practice [14]. Many of these alternatives are based on other types of simplifications of the objective function, respectively the Wasserstein distance. We just provide a select few examples: The so-called Radon barycenters and Sliced barycenters [9,39] are restricted to special instances (Radon barycenters are only practical for data on a grid, Sliced barycenters deal with support points of uniform mass), but provide favorable practical performance in low dimension. The idea is to use a Radon transform to obtain 1-dimensional projections of the support points to lines sampled randomly, from which an expectation of the Wasserstein distance can be devised. Further, a use of the simpler W_1 -distance instead of the W_2 -distance leads to the so-called Beckmann problem, which allows various efficient approaches [3,21,41].

1.2 Contributions

In this paper, we study LP-based approaches to the discrete barycenter problem. In Section 2, we introduce some notation and recall previous related work on linear programming for the problem. In Section 3, we present and discuss our main contributions.

First, we show that an optimal measure for Eq. (1), when restricted to the union of supports of the original measures, gives a tight 2-approximation for the barycenter problem (Theorem 1). This result has an immediate implication for some of the algorithms in the literature that compute an approximate barycenter for grid-structured data: If the computation is done over the underlying grid itself, the algorithm does not converge to an exact barycenter, but to a best approximation of it over the grid, which can give up to a 2-error.

Next, we exhibit that a restriction to the support of the original measures allows us to trade this small, provable approximation error for a dramatic improvement in the sizes of barycenters LPs – linear or quadratic instead of exponential: We obtain an LP-based 2-approximation algorithm that can be set up and solved in strongly polynomial time (Algorithm 1, Theorem 2). The algorithm finds a sparse approximate barycenter; to the best of the author’s knowledge, this is the first approximation algorithm for a *sparse* solution to the problem. In particular, this shows that the barycenter problem can be efficiently approximated *for any data*.

The output of Algorithm 1 may not allow for a non-mass splitting transport. (Recall that the existence of such a transport is a property of all exact barycenters and is important for many applications.) Next, we present a second algorithm that starts with an approximate barycenter as computed by Algorithm 1 and improves it to another measure for which there exists a non-mass splitting transport of lower cost, and prove that this computation also runs in strongly polynomial time (Algorithm 2, Theorems 3 and 4). This algorithm achieves the improvement by moving mass out of the union of original supports to a new, adapted support set. Both Algorithms 1 and 2 work for any input and do not require the a priori specification of a fixed support set.

Finally, we use the two algorithms as the building blocks of an iterative scheme alternating between them (Algorithm 3). We prove that it terminates with a 2-approximation with both sparse support and an associated non-mass splitting optimal transport at the same time (Theorem 5). The theoretical running time of this third algorithm remains open at this time; in practical computations we observe a low number of iterations (often just two to four) before termination. This behavior is reminiscent of the well-known k -means algorithm [28,32]. Further, while we prove that the 2-approximation bound for our algorithms is tight in theory, we have not observed more than a 20% error, respectively a multiplicative 1.2 error, in any of our computations.

In Section 4, we provide the necessary proofs and some examples. We conclude with sample computations and an analysis of the scaling of the algorithms in Section 5. We provide comparisons to exact, LP-based computations, and observe dramatic improvements in running time.

At the same time, one has to be very careful in a comparison with other methods in the literature, not only because of differences in input and desired output. Our algorithms have several favorable properties that come at a significant computational cost: Algorithm 1 already is an exact, sparse solution over the original support, and its result is further refined through Algorithms 2 and 3. Further, the algorithms are numerically stable, work for any data and without specification of a fixed support set for the solution. As expected, simpler settings (like entropy regularized input or Radon/Sliced barycenters) for grid-based data can lead to much faster running times – the output is a dense approximation over the original support. If purely interested in the speed of large-scale computations in practice, we only recommend the methods in this paper for sets of measures of small, overlapping support. We close the discussion with an example of this type, where scaling becomes linear and we are able to find solutions for thousands of measures. Such data is common in operations research applications that involve geographical locations.

2 Preliminaries

We begin by recalling some background on LP-based approaches to the discrete barycenter problem, following [2] and [34]. We are given a set of *discrete probability measures* P_1, \dots, P_N ,

i.e., they have finite support in \mathbb{R}^d and their total mass sums up to 1. For a simple wording, we call them *measures* in this paper, or *discrete measures* to stress the finite support. A set of support points with associated total mass less than 1 will be called a *partial measure*. We denote the support of P_i as $\text{supp}(P_i)$ and its size as $|P_i| = |\text{supp}(P_i)|$. Further, we are given a weight vector $\lambda = (\lambda_1, \dots, \lambda_N) \in \mathbb{R}_{>0}^N$ with $\sum_{i=1}^N \lambda_i = 1$.

The general definition of a Wasserstein barycenter refers to a measure \bar{P} on \mathbb{R}^d which satisfies Eq. (1), i.e.,

$$\phi(\bar{P}) = \sum_{i=1}^N \lambda_i W_2(\bar{P}, P_i)^2 = \inf_{P \in \mathcal{P}^2(\mathbb{R}^d)} \sum_{i=1}^N \lambda_i W_2(P, P_i)^2.$$

For discrete measures P_1, \dots, P_N , one can show [2] that all optimizers of Eq. (1) must be supported in the finite set $S \subset \mathbb{R}^d$ defined as

$$S := \left\{ \sum_{i=1}^N \lambda_i x_i : x_i \in \text{supp}(P_i) \right\}. \quad (2)$$

S is the set of all possible weighted centroids for a combination of support points with one from each measure P_i . Note that S does not have to overlap with any of the support sets $\text{supp}(P_i)$.

Letting $\mathcal{P}_S^2(\mathbb{R}^d) := \{P \in \mathcal{P}^2(\mathbb{R}^d) \mid \text{supp}(P) \subseteq S\}$, the infinite-dimensional problem in Eq. (1) can be solved by replacing the requirement $P \in \mathcal{P}^2(\mathbb{R}^d)$ with $P \in \mathcal{P}_S^2(\mathbb{R}^d)$ to obtain

$$\phi(\bar{P}) = \inf_{P \in \mathcal{P}_S^2(\mathbb{R}^d)} \sum_{i=1}^N \lambda_i W_2(P, P_i)^2. \quad (3)$$

This yields a finite-dimensional minimization problem, which can be solved by linear programming [2,10,14]:

Let P_1, \dots, P_N be a set of discrete measures and let $\text{supp}(P_i) = \{x_{ik} \mid k = 1, \dots, |P_i|\}$. Further, let P_0 be another (fixed) discrete measure and let $\text{supp}(P_0) = \{x_j \mid j = 1, \dots, |P_0|\}$. Finally, let d_{ik} be the mass of the point x_{ik} in P_i and d_j be the mass of the point x_j in P_0 . First, we can find the value of $\phi(P_0) = \sum_{i=1}^N \lambda_i W_2(P_0, P_i)^2$, i.e., the cost of an optimal transport from P_0 to all the P_i , by solving the following LP:

$$\begin{aligned} \min_y \quad & \sum_{i=1}^N \lambda_i \sum_{j=1}^{|P_0|} \sum_{k=1}^{|P_i|} \|x_j - x_{ik}\|^2 y_{ijk} && \text{(opt. transport)} \\ \text{subject to} \quad & \sum_{k=1}^{|P_i|} y_{ijk} = d_j, \quad \forall i = 1, \dots, N, \quad \forall j = 1, \dots, |P_0|, \\ & \sum_{j=1}^{|P_0|} y_{ijk} = d_{ik}, \quad \forall i = 1, \dots, N, \quad \forall k = 1, \dots, |P_i|, \\ & y_{ijk} \geq 0, \quad \forall i = 1, \dots, N, \quad \forall j = 1, \dots, |P_0|, \quad \forall k = 1, \dots, |P_i|. \end{aligned}$$

Note that we not only find an optimal objective function value $\phi(P_0)$, but an *(optimal) transport* $y = (y_{ijk})_{i \leq N, j \leq |P_0|, k \leq |P_i|}$ between P_0 and the P_1, \dots, P_N .

Next, the mass becomes part of the optimization. Instead of just searching for an optimal transport from a fixed measure P_0 , we use a set S_0 of *possible support points* with associated

variables that indicate the mass that is put on them. By introducing variables $z = (z_j)_{j \leq |S_0|}$ for the points in a given set $S_0 = \{x_j | j = 1, \dots, |S_0|\}$ to denote the possible mass at $x_j \in S_0$, we obtain an LP that both finds an optimal measure P_0 supported on S_0 , as well as the corresponding optimal transport to get an optimal value for $\phi(P_0) = \sum_{i=1}^N \lambda_i W_2(P_0, P_i)^2$:

$$\begin{aligned}
\min_{z,y} \quad & \sum_{i=1}^N \lambda_i \sum_{j=1}^{|S_0|} \sum_{k=1}^{|P_i|} \|x_j - x_{ik}\|^2 y_{ijk} && \text{(barycenter)} \\
\sum_{k=1}^{|P_i|} y_{ijk} = & z_j, \quad \forall i = 1, \dots, N, \quad \forall j = 1, \dots, |S_0|, \\
\sum_{j=1}^{|S_0|} y_{ijk} = & d_{ik}, \quad \forall i = 1, \dots, N, \quad \forall k = 1, \dots, |P_i|, \\
y_{ijk} \geq & 0, \quad \forall i = 1, \dots, N, \quad \forall j = 1, \dots, |S_0|, \quad \forall k = 1, \dots, |P_i|
\end{aligned}$$

Note that the variables z_j have to satisfy $z_j \geq 0$ and $\sum_{j=1}^{|S_0|} z_j = 1$ to correspond to a measure. But this is a direct consequence of satisfaction of the other constraints and $\sum_{i=1}^N d_{ik} = 1$ for all $i \leq N$, as the P_i are measures themselves. Thus, the above LP computes a measure represented by z and a corresponding optimal transport y . When choosing $S_0 = S$, the returned (z, y) represents a discrete barycenter by z and a corresponding optimal transport by y . For $S_0 \neq S$, we call the measure represented by z an S_0 -barycenter, an *approximation of the barycenter in S_0* , or when the context is clear simply an *approximate barycenter*.

Let us consider the size of LP (barycenter). It consists of $|S_0| + |S_0| \cdot \sum_{i=1}^N |P_i|$ variables and $N \cdot |S_0| + \sum_{i=1}^N |P_i|$ equality constraints. For the computation of a barycenter, we have $S_0 = S$. In this case, we get a worst-case bound of $|S_0| = \prod_{i=1}^N |P_i|$. Let now $|P_{\max}| = \max_{i=1, \dots, N} |P_i|$. If all measures have the same number of support points, we get $\sum_{i=1}^N |P_i| = N \cdot |P_{\max}|$ and $\prod_{i=1}^N |P_i| = |P_{\max}|^N$. So we have an LP of up to $|P_{\max}|^N + |P_{\max}|^N \cdot N \cdot |P_{\max}|$ variables and $N \cdot |P_{\max}|^N + N \cdot |P_{\max}|$ equality constraints.

A more refined analysis reveals that some of the variables and constraints can be redundant. For example, if the measures overlap in some of their support points, then $|S_0|$ and consequently the size of the LP becomes smaller. In fact, LP (barycenter) is always of polynomial size for data on a grid [10]. For data not a grid, we cannot rule out a scaling of the size of the LP for $S_0 = S$ that is exponential in N even if $|P_{\max}|$ is fixed, and a polynomial scaling in $|P_{\max}|$ even if N is fixed. The main reason why it was possible to compute an exact barycenter for the example in [2] with only 8 measures of 9 support points was the fact that all measures had the same small support, which had a dramatic effect in reducing $|S_0|$. This highlights the potential benefit from performing an approximate computation where one replaces S by a smaller set $|S_0|$.

The feasible regions of LPs (opt. transport) and (barycenter) are bounded, and thus standard arguments of linear programming show that there always exists an optimal vertex. In a vertex, an inclusion-maximal set of variables is set to 0. By a careful analysis of which of the variables z_j, y_{ijk} are equal to 0, it is possible to show a first favorable property: In contrast to the large number $|S|$ of possible support points, which can be up to $\prod_{i=1}^N |P_i|$, there always exists a barycenter that assigns nonzero mass to at most $\sum_{i=1}^N |P_i| - N + 1$ points [2].

Proposition 1. *Let P_1, \dots, P_N be discrete measures. Then for any weights $\lambda \in \mathbb{R}_{>0}^n$, there exists a barycenter \bar{P} of these measures such that*

$$|\bar{P}| \leq \sum_{i=1}^N |P_i| - N + 1. \quad (4)$$

We call a measure \bar{P} that satisfies $|\bar{P}| \leq \sum_{i=1}^N |P_i| - N + 1$ *sparse*. Using this wording, Proposition 1 states that there always exists a *sparse barycenter*. A proof is based on the existence of an optimal vertex of the polyhedron for LP (barycenter) [2,34]. The argument also works if a support set $S_0 \neq S$ is used. LP (barycenter) then optimizes the objective function in Eq. (1) over the set $\mathcal{P}_{S_0}^2(\mathbb{R}^d)$ of all measures P with support in S_0 . For these different support sets, we have the following generalization of Proposition 1.

Corollary 1. *Let P_1, \dots, P_N be discrete measures in \mathbb{R}^d , let $S_0 = \{x_j : j = 1, \dots, |S_0|\} \subset \mathbb{R}^d$, and let $\mathcal{P}_{S_0}^2(\mathbb{R}^d)$ be the set of all measures P with support in S_0 . Then for any weights $\lambda \in \mathbb{R}_{>0}^n$, there exists an approximate barycenter \bar{P}_0 in S_0 such that*

$$|\bar{P}_0| \leq \sum_{i=1}^N |P_i| - N + 1. \quad (5)$$

Further, for any barycenter \bar{P} it is possible to show the existence of a *non-mass splitting optimal transport* from \bar{P} to the P_1, \dots, P_N [2,34]. This means that for all $x_j \in \text{supp}(\bar{P})$ with mass d_j and for each i , there is exactly one k with $y_{ijk} = d_j$ for the corresponding variables in LP (opt. transport), while $y_{ijk'} = 0$ for all $k' \neq k$. So each support point of a barycenter only transports mass to exactly one support point in each measure. In this case, we say that a support point does not split mass or that a support point is *non-mass splitting*.

In fact, *any* optimal transport from a discrete barycenter \bar{P} to the corresponding set of measures is non-mass splitting. While this has not been stated explicitly in [2], it is not hard to prove: Recall that the (weighted) centroid c of a set of points x_1, \dots, x_n is the unique minimizer of a functional that measures the (weighted) summed-up squared Euclidean distances of a single point to all points in the set. This can be seen through a simple transformation

$$\sum_{i=1}^N \lambda_i \|(s + c) - x_i\|^2 = s^T s - c^T c + \sum_{i=1}^N \lambda_i x_i^T x_i,$$

which is minimal for $s^T s = 0$, so $s = 0$. If there was a barycenter support point splitting mass, it could be split into two (or more) centroids of support points in the measures of the same total mass, and the cost of transport would be strictly lower. We formally state this observation.

Proposition 2. *Let P_1, \dots, P_N be discrete measures, and let \bar{P} be a barycenter for these measures. Then any optimal transport from \bar{P} to P_1, \dots, P_N is non-mass splitting.*

3 Main Results

In this paper, we study approximations of the discrete barycenter problem where the set S , required to find an exact barycenter, is replaced by much smaller sets S_0 . This is motivated by the unfavorable scaling of LP (barycenter) with respect to $|S|$, respectively $|S_0|$; see Section 2. We here outline our main results, Section 4 provides the necessary proofs and some examples, and Section 5 a discussion of the scaling and some sample computations.

3.1 A strongly polynomial 2-approximation

Recall that the set of possible support points of a discrete barycenter is

$$S := \left\{ \sum_{i=1}^N \lambda_i x_i : x_i \in \text{supp}(P_i) \right\}, \quad (6)$$

which may consist of up to $\prod_{i=1}^N |P_i|$ points. This is a much larger number than the size of the union of supports of the measures

$$S_{\text{org}} := \bigcup_{i=1}^N \text{supp}(P_i), \quad (7)$$

which satisfies $|S_{\text{org}}| \leq \sum_{i=1}^N |P_i|$ with equality if and only if the supports are disjoint.

Note that the maximal size of S_{org} only barely exceeds the bound on the size of a sparsest-possible approximate barycenter in Proposition 1. Nonetheless, we can bound the approximation error from searching for an approximate barycenter in S_{org} , i.e., setting $S_0 = S_{\text{org}}$ in LP (barycenter), by a factor of two. This bound is tight.

Theorem 1. *Let \bar{P} be a barycenter and let \bar{P}_{org} be an approximate barycenter in S_{org} . Then*

$$\phi(\bar{P}_{\text{org}}) \leq 2 \cdot \phi(\bar{P})$$

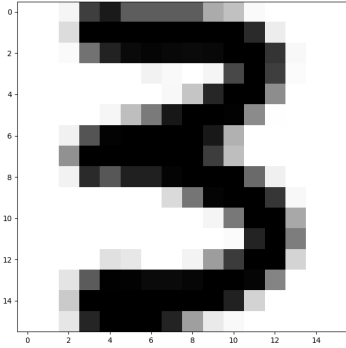
and this bound can become tight, i.e., there is a set of measures P_1, \dots, P_N and a set of weights $\lambda_1, \dots, \lambda_N$ for which $\phi(\bar{P}_{\text{org}}) = 2 \cdot \phi(\bar{P})$.

We formally denote the choice of S_{org} in LP (barycenter), as performed for Theorem 1, as Algorithm 1. The difference between the support for an exact barycenter and for this approximation is highlighted in Figure 1: The first two rows show four handwritten digits scanned into a 16×16 grid. (See [27] for some information on this data set.) These are the measures P_1, \dots, P_4 . The varying shades of grey indicate different masses at the support points of the grid (the darker, the larger the mass). The masses for each measure add up to 1. The bottom row depicts an exact barycenter and a 2-approximation in the original 16×16 grid (for all $\lambda_i = \frac{1}{4}$). The support grid for the exact barycenter is four times finer, a $(4 \cdot 16 - 3) \times (4 \cdot 16 - 3) = 61 \times 61$ grid.

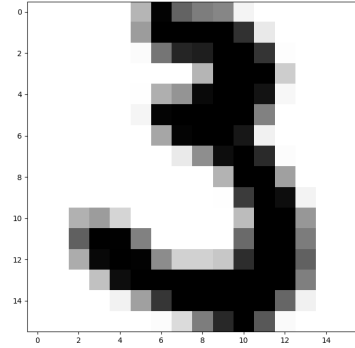
Note that Algorithm 1 is stated to compute an optimal vertex of the feasible region. This guarantees that the sparsity condition stated in Corollary 1 is satisfied, so the returned measure is not only an approximate barycenter in S_{org} , but also *sparse*. However, there are examples where any corresponding optimal transport splits mass, in contrast to Proposition 2; we exhibit such an example in Section 4.1. Summing up, the differences of Algorithm 1 and a solution of LP (barycenter) are the use of support S_{org} (as in Eq. (7)) and the search for an optimal vertex. For a convenient wording, we will say that Algorithm 1 is used with a given support S_0 as input when we require an optimal vertex, and not just any optimal solution, of LP (barycenter).

We close our discussion of Algorithm 1 by identifying its favorable running time.

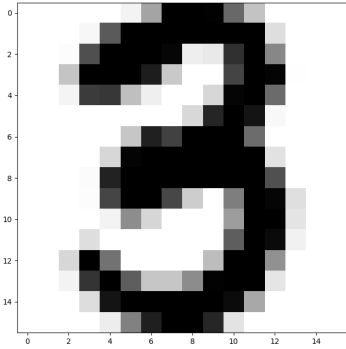
Theorem 2. *For all rational input, a 2-approximate barycenter can be computed in strongly polynomial time.*



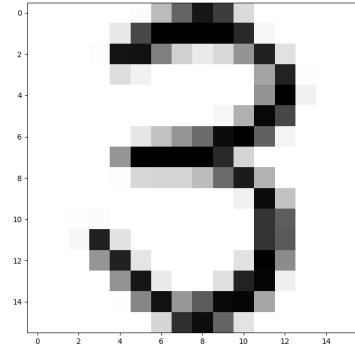
(1.1) Measure P_1



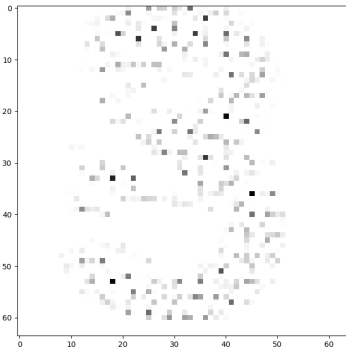
(1.2) Measure P_2



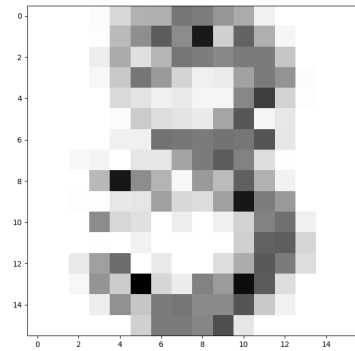
(1.3) Measure P_3



(1.4) Measure P_4



(1.5) Barycenter \bar{P}



(1.6) Approximate Barycenter \bar{P}_{org}

Fig. 1: Four measures P_1, \dots, P_4 supported on a 16×16 grid in the first two rows. The bottom row shows a barycenter \bar{P} and an approximate barycenter \bar{P}_{org} . While the support of \bar{P}_{org} lies in the original 16×16 grid, the support for \bar{P} lies in a four times finer grid.

Algorithm 1 Sparse 2-approximate barycenter in the original support

Input

- Measures $P_1, \dots, P_N \subset \mathbb{R}^d$, support $S_{\text{org}} = \bigcup_{i=1}^N \text{supp}(P_i)$
- $\lambda_1, \dots, \lambda_N > 0$ with $\sum_{i=1}^N \lambda_i = 1$

Algorithm

Compute an approximate barycenter \bar{P}_{org} in S_{org} as an optimal vertex (z, y) of

$$\begin{aligned} \min_{z, y} \quad & \phi(\bar{P}_{\text{org}}) := \sum_{i=1}^N \lambda_i \sum_{j=1}^{|S_{\text{org}}|} \sum_{k=1}^{|P_i|} \|x_j - x_{ik}\|^2 y_{ijk} \\ \text{subject to} \quad & \sum_{k=1}^{|P_i|} y_{ijk} = z_j, \quad \forall i = 1, \dots, N, \quad \forall j = 1, \dots, |S_{\text{org}}|, \\ & \sum_{j=1}^{|S_{\text{org}}|} y_{ijk} = d_{ik}, \quad \forall i = 1, \dots, N, \quad \forall k = 1, \dots, |P_i|, \\ & y_{ijk} \geq 0, \quad \forall i = 1, \dots, N, \quad \forall j = 1, \dots, |S_{\text{org}}|, \quad \forall k = 1, \dots, |P_i| \end{aligned}$$

and return z to represent \bar{P}_{org} and the corresponding optimal transport y .

A proof is based on exhibiting that LP (barycenter) is of strongly polynomial size, and that its numbers can be computed in strongly polynomial time. Strongly polynomial solvability of this LP then follows from the constraint matrix only having entries in $\{-1, 0, 1\}$; the numbers in the objective function and right-hand sides does not matter [44].

3.2 Recovery of Non-Mass Split

Next, we design an algorithm that begins with a (sparse) 2-approximate barycenter computed by Algorithm 1. The algorithm improves it to another measure supported on a subset of S (instead of S_{org}), for which there exists a non-mass splitting transport of lower cost, i.e., the approximation error can only become better. Algorithm 2 sums up the approach in pseudocode. In this section, we describe the algorithm in some detail; additional technical details are given in the proof of Theorem 3.

The algorithm greedily breaks up each support point (that splits mass) of the approximate barycenter into several non-mass splitting support points (Steps 1 – 3). In the end, all of the non-mass splitting support points are combined to a new measure (Step 4). The preprocessing performed in Step 2 guarantees that the non-mass split property for each support point in Step 3 transfers to the existence of a non-mass splitting transport for the new measure constructed in Step 4. Figure 2 shows a run of the algorithm, which is discussed in more detail as Example 1 at the end of the section.

Step 1. First, the approximate barycenter \bar{P}_{org} is broken up into disjoint parts; each part corresponds to a support point $s_l = x_{t_l}$ in the approximate barycenter. By construction, each P_i^l consists of those support points in P_i to which s_l transports mass. The mass of a support point in P_i^l equals the mass it receives as transport from s_l . In the end, we give new

indices to the support points in P_i^l and their masses for a simpler notation, so we do not have to refer to z or y in the subsequent steps.

Step 2. Step 2 (and Step 3) is based on the construction of so-called *lexicographically maximal* vectors. We call a vector $a = (a_1, \dots, a_n)$ *lexicographically larger* than a vector $b = (b_1, \dots, b_n)$ if there is an index $j \leq n$ such that $\sum_{i=1}^j a_i > \sum_{i=1}^j b_i$, while $\sum_{i=1}^l a_i \geq \sum_{i=1}^l b_i$ for all $l < j$. For example, the vector $a = (2, 2, 0, 1)$ is lexicographically larger than $b = (2, 1, 5, 10)$. Lexicographic maximality with respect to a set states that there is no lexicographically larger vector in the set. Note that the term gives rise to a total ordering.

The intuition for the construction of lexicographically maximal vectors is to resolve ties. This is necessary in two different settings: in Step 2, as much mass as possible is greedily shifted to support points of lower indices; in Step 3, a lexicographically decreasing sequence of weighted centroids is created from each support point. Together, these two steps make sure that all the weighted centroids that are merged to form \bar{P}' in Step 4 are distinct and only transport to a single support point in each measure, implying the existence of a non-mass splitting transport.

Step 2 iteratively transforms (d_1, \dots, d_r) to be lexicographically larger and larger, while retaining an approximate barycenter supported in $\text{supp}(\bar{P}_{\text{org}})$ (that is, the cost of an optimal transport does not increase). It does so via a greedy scheme, where mass is moved to support points in $\text{supp}(\bar{P}_{\text{org}})$ with the lowest indices, until this is not possible anymore. We call a (d_1, \dots, d_r) that is not altered by Step 2 *greedily lexicographically maximal*. Note that such a vector need not be lexicographically maximal among all approximate barycenters with the same support. The result of a run of Step 2 always is greedily lexicographically maximal; this is enough for our purposes.

The two loops for l and j establish an order for checking whether mass can be moved from s_l to s_j , while keeping optimality over $\text{supp}(\bar{P}_{\text{org}})$. The indices $q_i = \arg \max_{q \leq |P_i^l|} (s_j - s_l)^T x_{iq}^l$ selected in 2a) identify support points in the P_i^l that lie the furthest in direction of $s_j - s_l$. Their weighted centroid c is a maximizer of $\|c - s_l\|^2 - \|c - s_j\|^2$. This difference is bounded above by 0 because of optimality of \bar{P}_{org} . However, if $\|c - s_l\|^2 = \|c - s_j\|^2$, which is checked in 2b), then mass can be shifted from s_l to s_j to make (d_1, \dots, d_r) lexicographically larger, while keeping optimality. The remainder of 2b) is a technical description of this shift of mass.

Step 3. Next, we perform a (greedy) routine to spread out the mass of each s_l to several support points. We do so by picking a set of lexicographically maximal support points x_{iq}^l in each P_i^l (i.e., we pick an x_{iq}^l with a largest first coordinate, and among those one with a largest second coordinate, and so on). Then we move mass d_{\min} to the weighted centroid $c = \sum_{i=1}^N \lambda_i x_{iq}^l$, where d_{\min} is the minimal mass among the d_{iq}^l . Such a centroid, viewed as a partial measure with one support point, trivially has a non-mass splitting transport to the support points it was constructed from. We repeat this scheme until all of the mass of a support point has been spread out, then continue with the next support point.

Step 4. Finally, we combine the partial measures from Step 3 to a new measure. It is at least as good an approximation of an exact barycenter as \bar{P}_{org} . This is because in Step 3, for any chosen set of support points x_{iq}^l we put the corresponding mass on their weighted centroid, which is a best-possible choice (at least as good as transport from s_l).

We sum up the favorable properties of the algorithm in Theorem 3. In addition to the existence of a non-mass splitting transport, and keeping a 2-approximation error, we are able to bound the size of the support by the square of the bound in Proposition 1. We do *not* prove that the returned measure is an approximate barycenter (which implies optimality over the given support by definition). The associated non-mass splitting transport is trivial to construct, but we do *not* prove that this transport is optimal. Due to this, we have to be

careful in the wording of the following statements (Theorems 3 and 4). A detailed proof is given in Section 4.2.

Theorem 3. *Algorithm 2 returns a measure \bar{P}' supported on a subset of S with $\phi(\bar{P}') \leq 2 \cdot \phi(\bar{P})$ and there is a non-mass splitting transport realizing this bound. Further $|\bar{P}'| \leq (\sum_{i=1}^N |P_i| - N + 1)^2$.*

Algorithm 2 Recovery of non-mass split

Input

- Measures $P_1, \dots, P_N \subset \mathbb{R}^d$
- (sparse) 2-approximate barycenter \bar{P}_{org} and an optimal transport (z, y) (from Alg. 1)
- $\lambda_1, \dots, \lambda_N > 0$ with $\sum_{i=1}^N \lambda_i = 1$

Algorithm

1. **(Break up \bar{P}_{org} into parts for each support point)**

Let $\text{supp}(\bar{P}_{\text{org}}) = \{s_1, \dots, s_r\} = \{x_{t_1}, \dots, x_{t_r}\}$ with corresponding masses $d_1 = z_{t_1}, \dots, d_r = z_{t_r}$. For each $l \leq r$ and $i \leq N$, construct P_i^l (a set of support points with masses) by the rule:

$$y_{it_l k} > 0 \Rightarrow \text{add } x_{ik} \text{ to } \text{supp}(P_i^l) \text{ with mass } y_{it_l k}$$

Now assign indices for the P_i^l to obtain a notation $P_i^l = \{x_{i1}^l, \dots, x_{i|P_i^l|}^l\}$ with corresponding masses $d_{i1}^l, \dots, d_{i|P_i^l|}^l$ for all $l \leq r$ and $i \leq N$.

2. **(Make (d_1, \dots, d_r) greedily lexicographically maximal)**

For $l = r$ descending to $l = 1$

For $j = 1$ ascending to $j = l - 1$

a) For each $i \leq N$, identify an index $q_i = \arg \max_{q \leq |P_i^l|} (s_j - s_l)^T x_{iq}^l$. Then compute

the weighted centroid $c = \sum_{i=1}^N \lambda_i x_{iq_i}^l$ from the corresponding support points.

b) If $\|c - s_j\|^2 = \|c - s_l\|^2$ then

Identify the minimal mass $d_{\min} = \min_{i \leq N} d_{iq_i}^l$ among the $x_{iq_i}^l$.

Set $d_l = d_l - d_{\min}$ and $d_{iq_i}^l = d_{iq_i}^l - d_{\min}$ for all $i \leq N$.

For all $i \leq N$, if $d_{iq_i}^l = 0$, remove $x_{iq_i}^l$ from $\text{supp}(P_i^l)$ and reindex P_i^l and $d_{i1}^l, \dots, d_{i|P_i^l|}^l$.

For all $i \leq N$, add $x_{iq_i}^l$ to $\text{supp}(P_i^j)$ if it is not in it yet. In this case, $|P_i^j|$ increases by one and we index the support point as $x_{i|P_i^j|}^j$ (with $d_{i|P_i^j|}^j = 0$).

Let now p_i be such that $x_{ip_i}^j = x_{iq_i}^l$ for all $i \leq N$.

Set $d_j = d_j + d_{\min}$ and $d_{ip_i}^j = d_{ip_i}^j + d_{\min}$ for all $i \leq N$.

If $d_l > 0$, go back to a).

3. **(Spread out each support point to a set of weighted centroids)**

For $l = 1$ ascending to $l = r$

Create an empty partial measure \bar{P}^l .

a) For each $i \leq N$, identify the index q_i for a lexicographically maximal support point

$x_{iq_i}^l$ in P_i^l . Then compute the weighted centroid $c = \sum_{i=1}^N \lambda_i x_{iq_i}^l$.

b) Identify the minimal mass $d_{\min} = \min_{i \leq N} d_{iq_i}^l$ among the $x_{iq_i}^l$.

Set $d_l = d_l - d_{\min}$ and $d_{iq_i}^l = d_{iq_i}^l - d_{\min}$ for all $i \leq N$.

For all $i \leq N$, if $d_{iq_i}^l = 0$, remove $x_{iq_i}^l$ from $\text{supp}(P_i^l)$ and reindex P_i^l and $d_{i1}^l, \dots, d_{i|P_i^l|}^l$.

Add c to $\text{supp}(\bar{P}^l)$ with mass d_{\min} .

If $d_l > 0$, go back to a).

4. **(Combine a new measure)**

Combine the partial measures \bar{P}^l to a measure $\bar{P}' = \sum_{l=1}^r \bar{P}^l$. Return \bar{P}' .

Let us discuss a small example for Steps 2 – 4 of the algorithm.

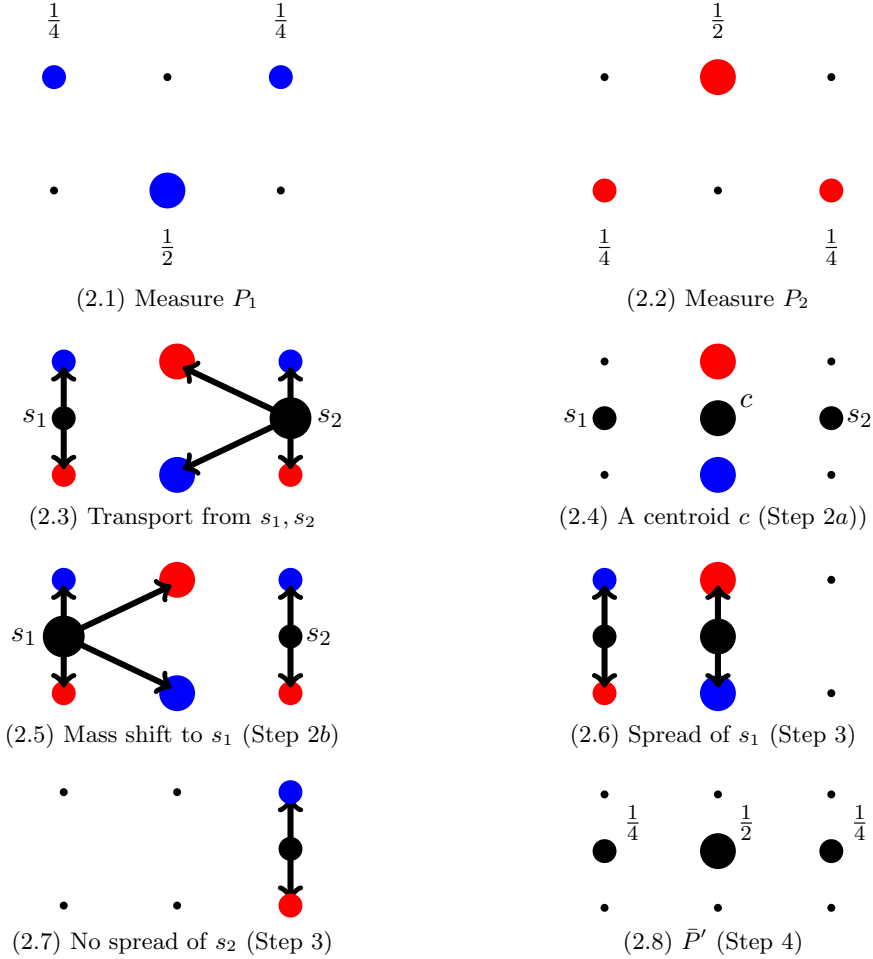


Fig. 2: Two measures P_1, P_2 in the top row and a run of Steps 2 – 4 of Algorithm 2 for given support points s_1, s_2 of mass $d_1 = \frac{1}{4}, d_2 = \frac{3}{4}$. Note $s_1, s_2 \notin S_{\text{org}}$, which may happen in later iterations of Algorithm 3, where Algorithm 2 is used as a subroutine.

Example 1. Consider the two measures P_1, P_2 depicted at the top of Figure 2 and let $\lambda_1 = \lambda_2 = \frac{1}{2}$. The volume of the filled circles represents the corresponding mass. They receive their mass transported from two fixed support points s_1, s_2 of mass $d_1 = \frac{1}{4}, d_2 = \frac{3}{4}$ (second row, left). Note that $s_1, s_2 \notin S_{\text{org}}$, which may happen in later iterations of Algorithm 3, where Algorithm 2 is used as a subroutine. (For this example, this does not matter.)

The two center points, which receive their mass from s_2 , have a centroid c that is equally far from s_1 and s_2 (second row, right). These two points would be selected in Step 2a) of Algorithm 2 and their mass shifted from s_2 to s_1 in Step 2b). Then $d_1 = \frac{3}{4}, d_2 = \frac{1}{4}$ (third row, left).

In Step 3, the mass of s_1 and s_2 is spread out to a set of centroids that transport to just a single support point in each measure. The result for s_1 is depicted in the third row (left). By lexicographically maximal choice of the points in the images, the central point of mass $\frac{1}{2}$ is constructed first, followed by the left one of mass $\frac{1}{4}$. s_2 is not changed, because it already is the centroid of a set of single support points in each measure (fourth row, left).

Algorithm 3 Iterative improvement

Input

- Measures $P_1, \dots, P_N \subset \mathbb{R}^d$
- $\lambda_1, \dots, \lambda_N > 0$ with $\sum_{i=1}^N \lambda_i = 1$

Algorithm

1. Compute a (sparse) 2-approximate barycenter \bar{P}_{org} in S_{org} (and an optimal transport) using Algorithm 1.
2. Use \bar{P}_{org} (and its transport) as input for Algorithm 2 to find a measure \bar{P}' .
If $\bar{P}' \neq \bar{P}_{\text{org}}$, set $S_{\text{org}} = \text{supp}(\bar{P}')$ and go back to 1. Else return \bar{P}' .

These measures are combined to form \bar{P}' in Step 4 (fourth row, right) and the algorithm stops. We actually found an exact barycenter, which is not the case in general. \square

We close our discussion of Algorithm 2 by showing that it runs in strongly polynomial time. The quite technical proof is given in Section 4.2.

Theorem 4. *For all rational input, a measure can be computed in strongly polynomial time that is a 2-approximation of a barycenter and for which there is a non-mass splitting transport realizing this bound.*

3.3 An Iterative Improvement

Finally, we combine Algorithms 1 and 2 to an iterative scheme, denoted as Algorithm 3. The algorithm begins by computing an approximate barycenter in S_{org} , as in Algorithm 1. Then Algorithm 2 is used to spread out its support points to not split mass anymore, which also improves the approximation error. The result is a new measure \bar{P}' . We set $S_{\text{org}} = \text{supp}(\bar{P}')$ and repeat Algorithm 1 to find an optimal approximate barycenter over this new support (in other words, an optimal vertex of LP (barycenter) over the new support is found). Then its support points are spread out again. This scheme is repeated until there is no improvement anymore.

After a finite number of iterations, the algorithm terminates with a sparse 2-approximate barycenter supported on a subset of S , and with a non-mass splitting optimal transport. This is a provable approximation that possesses both favorable properties of an exact barycenter.

Theorem 5. *Algorithm 3 returns an approximate barycenter \bar{P}' supported on a subset of S for which $\phi(\bar{P}') \leq 2 \cdot \phi(\bar{P})$, where \bar{P} is a barycenter, and there is a non-mass splitting optimal transport realizing this bound. Further $|\bar{P}'| \leq \sum_{i=1}^N |P_i| - N + 1$.*

We prove Theorem 5 in Section 4.3 and then discuss the approximation error in practice. We further provide an example that shows that the 2-approximation error remains tight. In Section 5 we conclude the paper with a discussion of the scaling and some observations on practical computations.

4 Proofs

4.1 Proofs for 3.1

We begin by proving Theorem 1, and in doing so proving the correctness of Algorithm 1.

Theorem 1 Let \bar{P} be a barycenter and let \bar{P}_{org} be an approximate barycenter in S_{org} . Then

$$\phi(\bar{P}_{\text{org}}) \leq 2 \cdot \phi(\bar{P})$$

and this bound can become tight, i.e., there is a set of measures P_1, \dots, P_N and a set of weights $\lambda_1, \dots, \lambda_N$ for which $\phi(\bar{P}_{\text{org}}) = 2 \cdot \phi(\bar{P})$.

Proof. We denote the mass of a support point c of a barycenter \bar{P} by d_c . By Proposition 2, there is an optimal transport such that c transports its mass to exactly one support point x_i in each P_i for all $i \leq N$. Due to optimality of \bar{P} , c is the weighted centroid $c = \sum_{i=1}^N \lambda_i x_i$ of these points. Recall the discussion after Corollary 1.

Each support point c contributes $d_c \cdot \sum_{i=1}^N \lambda_i \|c - x_i\|^2$ to the corresponding value $\phi(\bar{P})$. Let $s \in S_{\text{org}} = \bigcup_{i=1}^N \text{supp}(P_i)$ be such that $\|s - c\|^2$ is minimal and note that

$$\begin{aligned} \sum_{i=1}^N \lambda_i \|s - x_i\|^2 &= s^T s - 2c^T s + \sum_{i=1}^N \lambda_i x_i^T x_i = (s^T s - 2c^T s + c^T c) + \\ &+ (c^T c - 2c^T c + \sum_{i=1}^N \lambda_i x_i^T x_i) = \sum_{i=1}^N \lambda_i (\|s - c\|^2 + \|c - x_i\|^2) \end{aligned}$$

for any s . By choice of s and the fact that $x_i \in \text{supp}(P_i)$, we know $\|s - c\|^2 \leq \|c - x_i\|^2$ for all $i \leq N$, so we get

$$\sum_{i=1}^N \lambda_i \|s - x_i\|^2 = \sum_{i=1}^N \lambda_i (\|s - c\|^2 + \|c - x_i\|^2) \leq 2 \cdot \sum_{i=1}^N \lambda_i \|c - x_i\|^2.$$

Thus the transport from s , instead of from c itself, introduces an approximation error of 2, i.e., each such s contributes at most $2 \cdot d_c \sum_{i=1}^N \lambda_i \|c - x_i\|^2$ to the value $\phi(\bar{P}_{\text{org}})$. As this holds for all of the weighted centroids $c \in \text{supp}(\bar{P})$ and corresponding closest $s \in S_{\text{org}}$, this shows the existence of a measure $\bar{P}_{\text{org}} \in \mathcal{P}_{\text{org}}^2(\mathbb{R}^d)$ with approximation error 2 with respect to ϕ .

It remains to prove that the bound can be tight. We do so through a simple example. Let P_1, P_2 be two measures with a single support point $x_{11} \in \text{supp}(P_1)$, $x_{21} \in \text{supp}(P_2)$, each of mass 1. Then \bar{P} consists of the single support point $c = \lambda_1 x_{11} + \lambda_2 x_{21}$ of mass 1 and thus

$$\begin{aligned} \phi(\bar{P}) &= \lambda_1 \cdot \|c - x_{11}\|^2 + \lambda_2 \cdot \|c - x_{21}\|^2 = \lambda_1 \cdot \|\lambda_2(x_{21} - x_{11})\|^2 + \lambda_2 \cdot \|\lambda_1(x_{11} - x_{21})\|^2 = \\ &= \lambda_1 \lambda_2 (\lambda_2 + \lambda_1) \|x_{21} - x_{11}\|^2 = \lambda_1 \lambda_2 \|x_{21} - x_{11}\|^2. \end{aligned}$$

In contrast, the restriction of an approximate barycenter \bar{P}_{org} to possible support $S_{\text{org}} = \{x_{11}, x_{21}\}$ would give $\phi(\bar{P}_{\text{org}}) = \min\{\lambda_1, \lambda_2\} \cdot \|x_{21} - x_{11}\|^2$. Note $\lambda_1 \cdot \lambda_2 \geq \frac{1}{2} \min\{\lambda_1, \lambda_2\}$, with equality if and only if $\lambda_1 = \lambda_2 = \frac{1}{2}$. In this case, $\phi(\bar{P}_{\text{org}}) = 2 \cdot \phi(\bar{P})$. \square

The above 2-bound can only be tight in very special cases: Let $s \in S_{\text{org}}$ be such that $\|s - c\|^2$ is minimal for a given weighted centroid $c \notin S_{\text{org}}$ transporting to x_{i1}, \dots, x_{N1} with $x_{i1} \in P_i$. Then the approximation error 2 is not tight if $\|c - x_{i1}\|^2 \neq \|c - x_{j1}\|^2$ for any $i \neq j$. This is because then

$$\sum_{i=1}^N \lambda_i \|s - x_{i1}\|^2 = \sum_{i=1}^N \lambda_i (\|c - x_{i1}\|^2 + \|s - c\|^2) < 2 \cdot \sum_{i=1}^N \lambda_i \|c - x_{i1}\|^2,$$

as there has to be a $j \leq N$ with $\|c - x_{j1}\|^2 > \|s - c\|^2$.

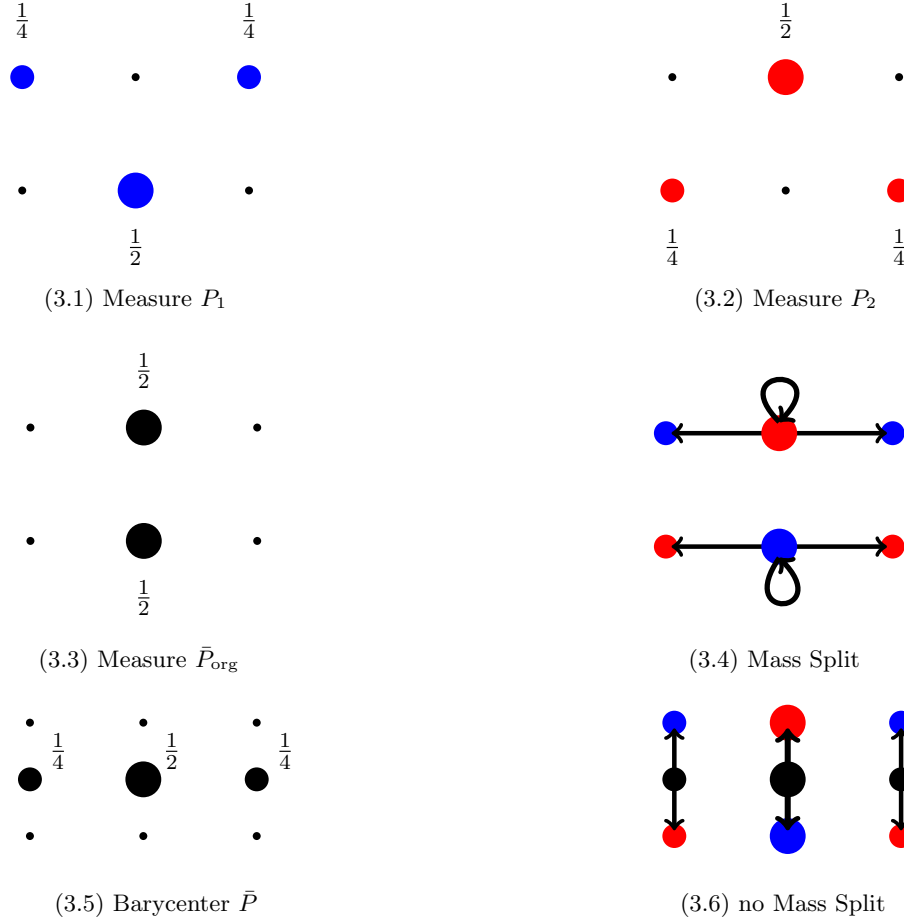


Fig. 3: Two measures P_1, P_2 in the top row. An optimal approximate barycenter $\bar{P}_{\text{org}} \in \mathcal{P}_{\text{org}}^2(\mathbb{R}^2)$ and the corresponding mass splitting transport in the second row. The exact barycenter and a corresponding non-mass splitting transport in the third row.

Further, it is easy to give examples where even an exact barycenter is contained in S_{org} . For example, take arbitrary P_1, \dots, P_N , compute their barycenter \bar{P} , and consider a new collection with $P_{N+1} = \bar{P}$. Then one has $\phi(\bar{P}_{\text{org}}) = \phi(\bar{P})$.

While \bar{P}_{org} is guaranteed to have sparse support, here is an example for a split of mass in the only optimal transport.

Example 2. We revisit the measures P_1 and P_2 used for Example 1. Consider Figure 3. Measure $\bar{P}_{\text{org}} \in \mathcal{P}_{\text{org}}^2(\mathbb{R}^d)$ (second row, left) is an optimal barycenter approximation in S_{org} . It consists of only two support points, while P_1 and P_2 have three support points. Thus, there exists a support point that splits mass in any transport, including the only optimal one (second row, right): The top support point of \bar{P}_{org} transports its mass $\frac{1}{2}$ in two parts $\frac{1}{4}$ to two support points of P_1 ; the same happens in the bottom part with respect to P_2 . Such a split of mass does not happen for an exact barycenter (third row). \square

Next, we prove that LP (**barycenter**) to find \bar{P}_{org} can be solved in strongly polynomial time.

Theorem 2 For all rational input, a 2-approximate barycenter can be computed in strongly polynomial time.

Proof. Recall that LPs are generally weakly polynomial-time solvable, i.e., the number of arithmetic operations necessary to solve them depends polynomially on the number of variables and constraints and polynomially on the absolute values of numbers in the input. However, it suffices to restrict this dependency to only the absolute value of numbers in the constraint matrix; the numbers in the objective function or the right-hand side of the constraints do not matter [44].

Note that the constraint matrix of LP (barycenter) for S_{org} only consists of entries in $\{-1, 0, 1\}$. For the claim of strongly polynomial solvability, it remains to prove that the number of variables and constraints of the LP is strongly polynomial in the size of the input, and that the numbers that appear in the objective function and right-hand sides can be computed from the original input in strongly polynomial time.

So let \mathcal{I} be an instance of the problem and let $|\mathcal{I}|$ be the number of bits to represent the input. Any representation of the input \mathcal{I} has to satisfy $|\mathcal{I}| \geq \sum_{i=1}^N |P_i| \geq N$. As $|S_0| = |S_{\text{org}}| \leq \sum_{i=1}^N |P_i| \leq |\mathcal{I}|$, LP (barycenter) indeed has a strongly polynomial number of constraints and variables.

The actual numbers that appear in the LP are of types λ_i , d_{ik} , or $\|x_j - x_{ik}\|^2$. The numbers λ_i and d_{ik} appear directly in the input, and so do the vectors x_j and x_{ik} . As we use rational input, $\|x_j - x_{ik}\|^2 = (x_j - x_{ik})^T(x_j - x_{ik})$ is a rational number derived by the sum over products of pairs of coefficients in x_j and x_{ik} . This implies that $\|x_j - x_{ik}\|^2$ can be computed in strongly polynomial time (polynomial in $\log x_j + \log x_{ik}$), as well as represented with a number of bits that is strongly polynomial in the number of bits of the original representation of x_j, x_{ik} . \square

4.2 Proofs for 3.2

We begin by proving Theorem 3.

Theorem 3 Algorithm 2 returns a measure \bar{P}' supported on a subset of S with $\phi(\bar{P}') \leq 2 \cdot \phi(\bar{P})$ and there is a non-mass splitting transport realizing this bound. Further $|\bar{P}'| \leq (\sum_{i=1}^N |P_i| - N + 1)^2$.

Proof. First, note that the P_i^l constructed in Step 1 satisfy $\text{supp}(P_i^l) \subset \text{supp}(P_i)$. Thus $\text{supp}(\bar{P}^l) \subset S$, and consequently $\text{supp}(\bar{P}') \subset S$. Further, $\bar{P}' = \sum_{l=1}^r \bar{P}^l$ is a measure. This is because $\sum_{l=1}^r d_l = \sum_{l=1}^r z_{t_l} = 1$, Step 2 does not change this sum, and the total mass in \bar{P}^l equals d_l by construction. So \bar{P}' is a measure supported in S .

Second, we prove correctness of Step 2. We will show that a greedily lexicographically maximal (d_1, \dots, d_r) is created while retaining an approximate barycenter in $\text{supp}(P_{\text{org}})$. In particular, we have to show that the objective function value $\phi(\bar{P}_{\text{org}})$ does not change during the shift of mass. For a simple wording, let \bar{P}_{lex} be the measure corresponding to (d_1, \dots, d_r) after Step 2. So we will prove $\phi(\bar{P}_{\text{org}}) = \phi(\bar{P}_{\text{lex}})$.

Let $x_{iq_i}^l \in P_i^l$ for $i \leq N$ and $c = \sum_{i=1}^N \lambda_i x_{iq_i}^l$, as in Step 2a). Then $\|c - s_l\| \leq \|c - s_j\|$ for all $j \neq l$. To see this, recall

$$\sum_{i=1}^N \lambda_i \|s - x_{iq_i}^l\|^2 = \sum_{i=1}^N \lambda_i (\|s - c\|^2 + \|c - x_{iq_i}^l\|^2),$$

as demonstrated in the proof of Theorem 1. If $\|c - s_l\| > \|c - s_j\|$, \bar{P}_{org} would not have been optimal.

By $q_i = \arg \max_{q \leq |P_i^l|} (s_j - s_l)^T x_{iq_i}^l$ in Step 2a), we pick the $x_{iq_i}^l$ such that for their weighted centroid $c = \sum_{i=1}^N \lambda_i x_{iq_i}^l$ the difference $\|c - s_l\|^2 - \|c - s_j\|^2 \leq 0$ is maximized. Only if $\|c - s_l\|^2 = \|c - s_j\|^2$, mass is shifted from s_l to s_j . But this implies that the approximation error does not change, because then

$$\sum_{i=1}^N \lambda_i \|s_j - x_{iq_i}^l\|^2 = \sum_{i=1}^N \lambda_i (\|s_j - c\|^2 + \|c - x_{iq_i}^l\|^2) = \sum_{i=1}^N \lambda_i \|s_l - x_{iq_i}^l\|^2.$$

Thus, the objective function value does not change during Step 2; we have $\phi(\bar{P}_{\text{org}}) = \phi(\bar{P}_{\text{lex}})$.

By definition of the running indices l and j , mass can only be moved from support points of larger index l to support points of smaller index j . For each pair of l and j , we repeat this shift of mass until there is no weighted centroid with $\|c - s_l\| = \|c - s_j\|$ anymore. Due to decreasing l in the outer loop and increasing j in the inner loop, (d_1, \dots, d_r) is transformed to be greedily lexicographically maximal and the corresponding measure remains an approximate barycenter.

Next, we prove correctness of Steps 3 and 4. We show that $\phi(\bar{P}_{\text{org}}) \geq \phi(\bar{P}')$. Further, we show that for each constructed partial measure \bar{P}^l there is a non-mass splitting transport to the P_i^l , and that they combine to a \bar{P}' that allows for a non-mass splitting transport that is at least as good as an optimal transport for \bar{P}_{org} . Finally, we show $|\bar{P}'| \leq (\sum_{i=1}^N |P_i| - N + 1)^2$.

Recall that in Step 3, the mass at each s_l is spread out to a set of weighted centroids to obtain \bar{P}^l . For $x_{iq_i}^l \in P_i^l$ for all $i \leq N$ and $c = \sum_{i=1}^N \lambda_i x_{iq_i}^l$ their weighted centroid, we see $\sum_{i=1}^N \lambda_i \|c - x_{iq_i}^l\|^2 \leq \sum_{i=1}^N \lambda_i \|s_l - x_{iq_i}^l\|^2$, independently of how the $x_{iq_i}^l$ are picked from P_i^l . By construction of \bar{P}' from the \bar{P}^l (Step 4), this already implies $\phi(\bar{P}') \leq \phi(\bar{P}_{\text{org}})$. The algorithm started with a 2-approximation, and thus it is guaranteed to return a \bar{P}' with $\phi(\bar{P}') \leq 2 \cdot \phi(\bar{P})$.

The existence of a non-mass splitting transport from \bar{P}' to P_1, \dots, P_N , and the fact that this transport realizes the above bound, is a consequence of two reasons. First, each \bar{P}^l itself allows for a non-mass splitting transport to the P_i^l by lexicographically maximal choice of the $x_{iq_i}^l$ in Step 3a): Due to this choice, the first constructed weighted centroid c is lexicographically maximal among all (possible) weighted centroids that can be constructed from any x_{iq}^l in the P_i^l . Further, by reducing the mass at each used support point by d_{\min} in Step 3b), at least one of the $d_{iq_i}^l$ becomes 0. The corresponding support point is removed from P_i^l (followed by some reindexing) and thus cannot be used for the construction of weighted centroids in further iterations. Thus the second centroid constructed in the inner loop is lexicographically strictly smaller than the first one. The same holds for all subsequent ones.

Second, any two partial measures $\bar{P}^{l_1}, \bar{P}^{l_2}$ from Step 3 satisfy $\text{supp}(\bar{P}^{l_1}) \cap \text{supp}(\bar{P}^{l_2}) = \emptyset$ for $l_1 \neq l_2$, because of the earlier preprocessing in Step 2: Weighted centroids that would be equally distant from both s_{l_1} and s_{l_2} cannot exist, because this would have caused a shift of mass to the lower index in Step 2 to create a lexicographically larger (d_1, \dots, d_r) . Summing up, \bar{P}' consists of a set of distinct support points, for which it is trivial to give a non-mass splitting transport to the P_i that is at least as good as an optimal transport for \bar{P}_{org} : This transport just sends the full mass of each support point in \bar{P}' to the support points in the P_i that were used for its construction.

The removal of at least one support point from a P_i^l in Step 3b) implies that there are at most $\sum_{i=1}^N |P_i^l| - N + 1$ runs of 3a) and 3b) to construct a P^l : The 'go back to a)' statement is applied while $d_l > 0$; this is the case while there still is a support point in a P_i^l with

mass on it. In the final run of Steps 3a) and 3b) for each P^l , all the P_i^l have precisely one support point with the same mass left. This gives the claimed bound, and in particular $|P^l| \leq \sum_{i=1}^N |P_i^l| - N + 1$.

Due to $|P_i^l| \leq |P_i|$ and $|\bar{P}_{\text{org}}| \leq \sum_{i=1}^N |P_i| - N + 1$, we obtain

$$|\bar{P}'| = \sum_{l=1}^{|\bar{P}_{\text{org}}|} |\bar{P}^l| \leq \sum_{l=1}^{|\bar{P}_{\text{org}}|} \left(\sum_{i=1}^N |P_i^l| - N + 1 \right) \leq \sum_{l=1}^{|\bar{P}_{\text{org}}|} \left(\sum_{i=1}^N |P_i| - N + 1 \right) \leq \left(\sum_{i=1}^N |P_i| - N + 1 \right)^2.$$

Thus \bar{P}' satisfies all the claimed properties. \square

Next, we prove that Algorithm 2 runs in strongly polynomial time.

Theorem 4 *For all rational input, a measure can be computed in strongly polynomial time that is a 2-approximation of a barycenter and for which there is a non-mass splitting transport realizing this bound.*

Proof. We consider the running time of each part of the algorithm. For readability, we say ‘polynomial’ in this proof in place of ‘strongly polynomial in the bit size of the input’. We use ‘linear’ and ‘quadratic’ to refer to the bit size of the input, too. Note that N , the $|P_i|$, and the dimension d are all bounded above by the bit size of the input.

In Step 1, the input for the subsequent steps is created. By sparsity of \bar{P}_{org} , $r \leq \sum_{i=1}^N |P_i| - N + 1$. For each of the r support points s_l , N images P_i^l with $|P_i^l| \leq |P_i|$ are created. In the application of the rule, each $y_{it_l k}$ has to be processed (at most) once. For each $y_{it_l k}$, a single comparison and a fixed number of elementary operations suffices to update the support point and mass in P_i^l . In total, data structures of polynomial size are created in polynomial time.

Step 2 is the preprocessing of (d_1, \dots, d_r) to be greedily lexicographically maximal. For each pair of support points s_l, s_j with $j < l$, we perform the inner part of the loop. Finding q_i in 2a) can be done by considering all $x_{iq}^l \in P_i^l$ exactly once and comparing the inner products $(s_j - s_l)^T x_{iq}^l$. This is possible in linear time. c is created by the scaling and the sum of N rational d -dimensional vectors.

Step 2b) begins with the computation of $c - s_j$ and $c - s_l$, then computes $\|c - s_j\|^2 = (c - s_j)^T (c - s_j)$ and $\|c - s_l\|^2 = (c - s_l)^T (c - s_l)$, and then compares the two values. This is possible in quadratic time. Picking the minimal mass among the x_{iq}^l is possible in linear time, and so is the update of the masses, the set operations on P_i^l and P_i^j , and the reindexing. By this update, $|P_i^l|$ is reduced by at least one, so the ‘go back to a’ statement is followed not more than $|P_i^l|$ times. Summing up, Step 2 runs in polynomial time.

Step 3 performs the spreading of the r support points. Picking a lexicographically maximal support point x_{iq}^l in 3a) can be done by considering all support points in P_i^l once. One saves the current best support point and compares each other support point with respect to their lexicographic order. For identifying the lexicographic order of a pair of d -dimensional support points, (at most) all d of their coefficients have to be compared to each other. This is possible in linear time. Again, c is created through the scaling and the sum of N rational d -dimensional vectors.

In 3b), we pick the minimal mass among the x_{iq}^l used for the construction of c , which can be done in linear time. The same holds for the update of masses, the set operations on P_i^l , and the reindexing. By this update, the size of one of the $|P_i^l|$ is reduced by at least one, so the ‘go back to a’ statement is followed not more than $\sum_{i=1}^N |P_i^l|$ times; more precisely,

there are at most $|P_i^l| - N + 1$ runs of 3a) and 3b) for each l . Summing up, the construction of each \bar{P}^l runs in polynomial time, and so does the construction of all the \bar{P}^l .

In Step 4, the partial measures \bar{P}^l are combined to obtain \bar{P}' . This is the construction of a measure with the appropriate mass put on at most $|\bar{P}'| \leq (\sum_{i=1}^N |P_i| - N + 1)^2$ support points. Each of these support points is just a copy of a support point in one of the \bar{P}^l . Thus, all steps run in polynomial time, which proves the claim. \square

4.3 Proofs for 3.3

We begin with a proof of Theorem 5.

Theorem 5 *Algorithm 3 returns an approximate barycenter \bar{P}' supported on a subset of S for which $\phi(\bar{P}') \leq 2 \cdot \phi(\bar{P})$, where \bar{P} is a barycenter, and there is a non-mass splitting optimal transport realizing this bound. Further $|\bar{P}'| \leq \sum_{i=1}^N |P_i| - N + 1$.*

Proof. First, recall that the output \bar{P}' of Algorithm 2 (Step 2) always satisfies $\text{supp}(\bar{P}') \subset S$. Further, Algorithm 2 will always return a measure that has a corresponding non-mass splitting transport. As \bar{P}_{org} from Algorithm 1 (Step 1) is not changed in the final iteration, neither is its optimal transport, so the returned non-mass splitting transport is also optimal. Next, note all approximate barycenters \bar{P}_{org} computed in Step 1 have a support that satisfies $|\bar{P}_{\text{org}}| \leq \sum_{i=1}^N |P_i| - N + 1$. This holds because Algorithm 1 finds a vertex of the feasible region, which guarantees the sparsity bound from Corollary 1 is satisfied [2]. This transfers to the sparsity of \bar{P}' returned by Algorithm 3.

It remains to prove termination of Algorithm 3 and the error bound. We will do so by showing that $\phi(\bar{P}') < \phi(\bar{P}_{\text{org}})$ if $\bar{P}' \neq \bar{P}_{\text{org}}$ for $\bar{P}_{\text{org}}, \bar{P}'$ from the same iteration. This leads to a strictly decreasing sequence of values $\phi(\bar{P}')$ as long as the algorithm keeps running. The first approximate barycenter in this sequence already is a 2-approximation and it can only become better throughout the run. This immediately gives $\phi(\bar{P}') \leq 2 \cdot \phi(\bar{P})$. At the end of each Step 2, we update $S_{\text{org}} = \text{supp}(\bar{P}') \subset S$ before going back to Step 1, where an exact optimum over this new support, a subset of S , is computed. Because of this, and the fact that there are only finitely many subsets of S , the sequence of values $\phi(\bar{P}')$ is finite.

Now, it only remains to prove that $\phi(\bar{P}') < \phi(\bar{P}_{\text{org}})$ if $\bar{P}' \neq \bar{P}_{\text{org}}$. We begin by considering Step 3 of Algorithm 2. Assume P_i^l consists of a single support point x_{i1}^l for all $i \leq N$. Then the unique barycenter \bar{P}^l of the P_i^l is the weighted centroid $c = \sum_{i=1}^N \lambda_i x_{i1}^l$. In this case we can denote the cost of transport from P^l to all the P_i^l by $\phi(\bar{P}^l) = d_l \cdot \sum_{i=1}^N \lambda_i \|c - x_{i1}^l\|^2$. For all $s \neq c$, we get

$$\phi(\bar{P}^l) = d_l \cdot \sum_{i=1}^N \lambda_i \|c - x_{i1}^l\|^2 < d_l \cdot \sum_{i=1}^N \lambda_i \|s - x_{i1}^l\|^2.$$

Note that for general P_i^l , in Step 3 of Algorithm 2, \bar{P}^l is constructed as a set of weighted centroids c of support points x_{iq}^l to which these centroids c transport. These are the ‘building blocks’ of the general \bar{P}^l . Thus $\phi(\bar{P}^l) \leq \sum_{i=1}^N \lambda_i \sum_{q=1}^{|P_i^l|} d_{iq}^l \cdot \|s_l - x_{iq}^l\|^2$.

Informally, it is at least as costly to transport to the measures P_i^l from the support point s_l as from the set of weighted centroids (with appropriate masses) constituting \bar{P}^l . Equality in the above can only hold if the single support point s_l itself already is the weighted centroid of single-support point measures P_1^l, \dots, P_N^l . But this means that Step 3 of Algorithm 2 just copies s_l with mass d_l to \bar{P}^l . The algorithm stops when $\bar{P}' = \bar{P}_{\text{org}}$. By $\phi(\bar{P}') = \sum_{l=1}^r \phi(\bar{P}^l)$,

this means all s_l have to satisfy $\phi(\bar{P}^l) = \sum_{i=1}^N \lambda_i \sum_{q=1}^{|P_i^l|} d_{iq}^l \cdot \|s_l - x_{iq}^l\|^2$. So all s_l are already the weighted centroids of their single-support measures P_i^l .

Further, note that when a shift of mass from s_l to s_j with $j < l$ happens in Step 2 of Algorithm 2, then Step 3 is guaranteed to find a strictly better transport than before: there exists a set of support points that, before the shift, receive transport from s_l , but have a weighted centroid $c \neq s_l$. Such a set of support points would be moved from P_i^l to P_i^j (and at least one of the support points was not associated to s_j before). Then s_j splits mass and, in the following Step 3, the cost of transport is strictly improved; see above.

Thus $\phi(\bar{P}') < \phi(\bar{P}_{\text{org}})$ if $\bar{P}' \neq \bar{P}_{\text{org}}$ and \bar{P}_{org} remains unchanged in the final run of Algorithm 2. So the final iteration of Algorithm 3 satisfies $\bar{P}' = \bar{P}_{\text{org}}$. \square

We take a closer look at the approximation error of Algorithm 3. It begins by computing a 2-approximate barycenter \bar{P}_{org} (in the first run of Step 1) and then improves it iteratively to obtain \bar{P}' . An exact barycenter \bar{P} can be rounded to the support S_{org} by solving the least-squares many-to-one matching

$$\bar{P}_r = \arg \min_{P_r \in \mathcal{P}_{\text{org}}^2(\mathbb{R}^d)} W_2(P_r, \bar{P})^2. \quad (8)$$

We call \bar{P}_r a ‘rounded’ barycenter. In the following, we distinguish four different measures: \bar{P} is an exact barycenter, \bar{P}_r is a rounded barycenter (rounded from \bar{P}), \bar{P}_{org} is an approximate barycenter in $\mathcal{P}_{\text{org}}^2(\mathbb{R}^d)$, and \bar{P}' is the solution of Algorithm 3. By optimality of \bar{P} and \bar{P}_{org} with respect to ϕ in their respective support, we obtain

$$\phi(\bar{P}) \leq \phi(\bar{P}') \leq \phi(\bar{P}_{\text{org}}) \leq \phi(\bar{P}_r).$$

We are particularly interested in the gap between $\phi(\bar{P})$ and $\phi(\bar{P}')$. Theorem 1 states $\phi(\bar{P}_{\text{org}}) \leq 2 \cdot \phi(\bar{P})$. However, the proof of Theorem 1 actually tells us that $\phi(\bar{P}_r) \leq 2 \cdot \phi(\bar{P})$. Thus the whole sequence of inequalities is bounded by a total approximation factor of 2. This implies that if $\alpha \phi(\bar{P}') = \phi(\bar{P}_{\text{org}})$ for some $\alpha \geq 1$, then $\phi(\bar{P}') \leq \frac{2}{\alpha} \phi(\bar{P})$.

In practice, one obtains a strictly better approximation factor than 2 for essentially all real-world problems using Algorithm 3. But there exist worst-case examples, such as the following, that show the bound is tight.

Example 3. Consider the example depicted in Figure 4. Four measures P_1, \dots, P_4 are shown in the top row, P_2, P_3 are depicted in the center. Note $P_2 = P_3$. Each of the measures consists of two support points of mass $\frac{1}{2}$. This time we give coordinates: P_1 is supported on $(-\epsilon, 0)$ and $(\epsilon, 1)$, P_2 and P_3 are supported on $(0, 0)$ and $(0, 1)$, and P_4 is supported on $(-\epsilon, 1)$ and $(\epsilon, 0)$, where $\epsilon > 1$. For increasing ϵ , the horizontal distance of the support points of P_1 and P_4 to those of P_2, P_3 increases proportionally (second row).

Let $\lambda_i = \frac{1}{4}$ for $i = 1, \dots, 4$. Independently of ϵ , an approximate barycenter \bar{P}_{org} in S_{org} is identical to $P_2 = P_3$, (third row, left). A corresponding optimal transport sends the mass to the support points in the same ‘layer’ (third row, middle). Note that the support points are already the (weighted) centroids of the points they transport to, and that the transport is non-mass splitting. Because of this, Algorithm 3 stops without any change to \bar{P}_{org} at the end of the first iteration.

The cost of transport for \bar{P}_{org} is $\phi(\bar{P}_{\text{org}}) = \frac{1}{4} \cdot 2\epsilon^2 = \frac{1}{2}\epsilon^2$. (Recall $\lambda_i = \frac{1}{4}$ for all i .) An exact barycenter \bar{P} (third row, right) and a corresponding optimal transport (fourth row) are strictly better. The coordinates for the two support points are $(-\frac{1}{2}\epsilon, \frac{3}{4})$ and $(\frac{1}{2}\epsilon, \frac{1}{4})$. The

cost of transport is $\phi(\bar{P}) = \frac{1}{4} \cdot (\frac{3}{4} + \epsilon^2) = \frac{3}{16} + \frac{1}{4}\epsilon^2$. (Note that flipping this barycenter along the vertical axis gives another, mirrored one.) For $\epsilon \rightarrow \infty$,

$$\frac{\phi(\bar{P}_{\text{org}})}{\phi(\bar{P})} = \frac{\frac{1}{2}\epsilon^2}{\frac{3}{16} + \frac{1}{4}\epsilon^2} \rightarrow 2.$$

Thus the error bound goes to 2. \square

5 Sample Computations and Scaling

We implemented Algorithms 1, 2, and 3 in the Julia language ([6,29]) using Clp as linear programming solver. The algorithms were run on a standard laptop (Win 10, 32GB memory, i7-6820).

In our implementation, we use some tweaks for a practical speed-up of Algorithm 3: First, we perform Step 3 of Algorithm 2 as the exact computation of a barycenter \bar{P}^l when the number of support points to which a given s_l transports is low (below $2N$). This leads to a better approximation bound for \bar{P}' at the end of each iteration of Algorithm 3 and a lower number of iterations overall. Further, this leads to a smaller support for the LPs in later iterations. In particular, this is valuable for the start of the second iteration, where S_{org} is replaced by the possibly much larger $\text{supp}(\bar{P}')$, and any reduction in the size of this new support is helpful. In later iterations, the supports do not change a lot anymore and can simply be updated. While each run of Algorithm 2 takes slightly longer with this approach, the running time remains negligible compared to Step 1 in each iteration. We observed a noticeable positive impact, dropping the total running time by about 22% on average.

Second, we explicitly construct the associated transport devised in Algorithm 2 and use it for a warm-start of the subsequent Step 1 of Algorithm 3: through this, we are able to start with a feasible vertex of the new LP, which itself is already almost optimal. Only few primal Simplex steps are necessary to get to the exact optimum over the new support. This is a crucial part of the implementation, as the LPs in later iterations can have millions of variables and otherwise would be slow to solve. Both of these tweaks do not affect our theoretical running time bounds for Algorithms 2 and 3.

Our computations are on two types of data: the MNIST database of handwritten digits (widely-used for benchmarking) [27] for a grid-structured setting, as well as the firehouse example from [2] for data in general position, i.e., where S would be exponentially-sized. Note that the algorithms in this paper works on any data, and for any choice of λ . Working outside of a grid setting, differing masses on the support points, or a non-uniform weight vector makes most of the algorithms in the literature impractical.

Our goal is to identify for which data the practical performance of the algorithms matches the favorable theoretical running time bounds. As we will see, it is data *not* on a grid, with a small support and a large number of measures, that forms a best-case scenario. (We also treat the less favorable grid setting in detail, for the sake of completeness.) We start with some sample runs for both types of data and then turn to the scaling with respect to the number of measures and size of the support.

5.1 Sample runs of Algorithm 3

We begin by exhibiting a sample run of Algorithm 3 in a grid setting, using the four digits representing number six in a 16×16 grid depicted in Figure 5. They have a barycenter depicted at the bottom of the figure (for all $\lambda_i = \frac{1}{4}$).

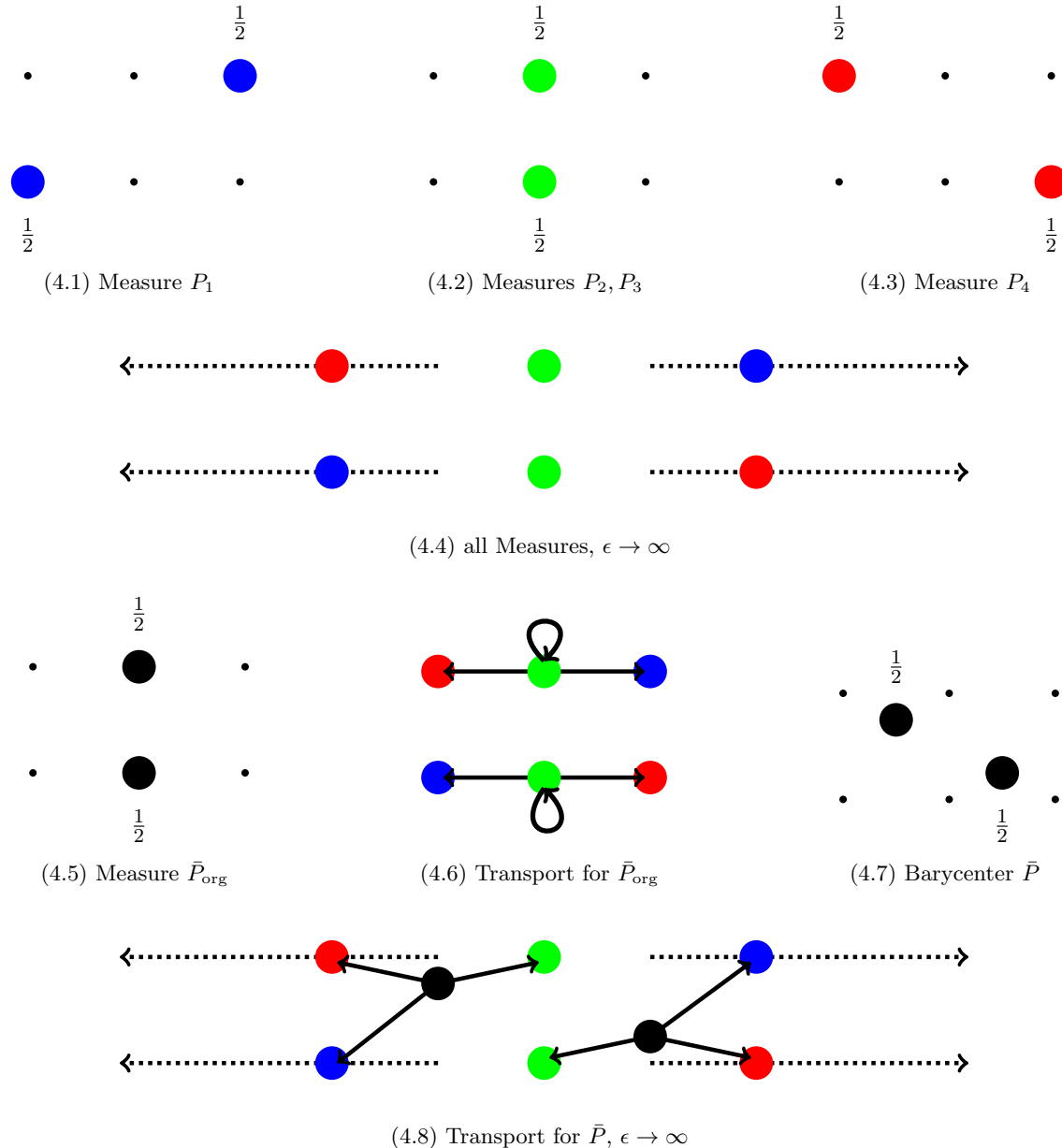


Fig. 4: Four measures P_1, \dots, P_4 (depicted for $\epsilon = 1$) in the first row. Note $P_2 = P_3$. For increasing ϵ , the horizontal distance of the support of P_1 and P_4 to $P_2 = P_3$ increases (second row). An approximate barycenter \bar{P}_{org} in S_{org} , corresponding transport, and an exact barycenter \bar{P} (all depicted for $\epsilon = 1$) in the third row. The transport for \bar{P} in the fourth row. Algorithm 3 returns \bar{P}_{org} . For $\epsilon \rightarrow \infty$, $\frac{\phi(\bar{P}_{\text{org}})}{\phi(\bar{P})} \rightarrow 2$, i.e., the error goes to 2.

Figure 6 shows the stages of a run of Algorithm 3 for this input. Each row shows one of the iterations. The approximate barycenter in the original support is already a 1.142-approximation of the exact barycenter (top left), i.e., $\phi(\bar{P}_{\text{org}}) \leq 1.142 \cdot \phi(\bar{P})$, which we denote as an additive 14.2%-error in the figure. The first split-up using Algorithm 2 (Steps 2 to 4) gives an improvement to a 4.3%-error (top right). This is further improved to a 2.0%-error (in Step 1 of Iteration 2) by computing an optimum in the support of the previous approximation (bottom left). Now the algorithm terminates, because all of the support points of this approximate barycenter are already the weighted centroids of the support points to which they transport mass, and there is no mass split.

Algorithm 3 completes in about 10 seconds on average for a set of four measures (9.6 seconds for the above example). In contrast, the computation of an exact barycenter takes roughly 120 seconds.

Next, we perform a sample run for data in general position. Here we begin with the input for the computations in [2]. There are 8 measures with the same 9 support points of varying masses. Figure 7 shows two of the measures. Circles of larger radius indicate higher mass.

Figure 8 shows the first \bar{P}_{org} and the result of the first run of Algorithm 2. The approximate barycenter in the original support is a 1.102-approximation of the exact barycenter, i.e., there is a 10.2%-error. This is improved to a 1.9%-error in the split-up using Algorithm 2. The second iteration of Algorithm 3 does not improve the solution anymore and the algorithm terminates.

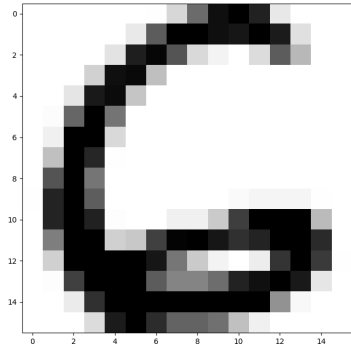
This run completes in about 0.8 seconds. In contrast, despite the common support of all measures, the set S is of exponential size, which makes the computation of an exact barycenter very hard: the LP for an exact computation has 939510 variables and 103032 constraints and takes roughly 500 seconds to solve [2].

Observations. Both of these sample runs are representative in a couple of ways. The approximation error for \bar{P}_{org} and the first improvement to \bar{P}' using Algorithm 2 are much better than the theoretical bound of 2. In the computations in Section 5.2, we have not encountered a run with an approximation error worse than 19% for the initial \bar{P}_{org} or 8.7% for the initial improvement to \bar{P}' . The improvement between \bar{P}_{org} and \bar{P}' in the first iteration is significant and should always be done in practical computations. However, the additional iterations of Algorithm 3 only perform minor improvements on the approximation factor. In fact, the example in Figure 6 was one of the larger improvements obtained after the first iteration, in all our computations.

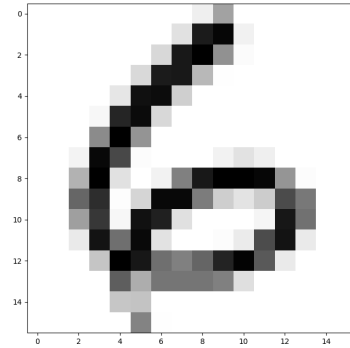
Only two parts contribute significantly to the total running time of Algorithm 3: the first run of Algorithm 1 and the setup of the LP for Step 1 in the second iteration. Only the first LP is run in full; the later LPs can be warm-started to solve in just a few Simplex iterations. Also, the setup of LPs in iterations 3 or later is a simple update from the previous iteration. The split-up of mass in Algorithm 2 is negligible in running time - the proof of Theorem 4 lays out the few elementary operations to perform it.

Of course, the initial run of Algorithm 1 is unavoidable in all situations. The setup of the second LP can be computationally expensive, because S_{org} is replaced by the larger $\text{supp}(\bar{P}')$. However, we observed that in practice $|\bar{P}'|$ does not only satisfy the guaranteed bound $|\bar{P}'| \leq (\sum_{i=1}^N |P_i| - N + 1)^2$ (Theorem 3), but remains close to $\sum_{i=1}^N |P_i| - N + 1$, the bound for $|\bar{P}_{\text{org}}|$ (Theorem 5).

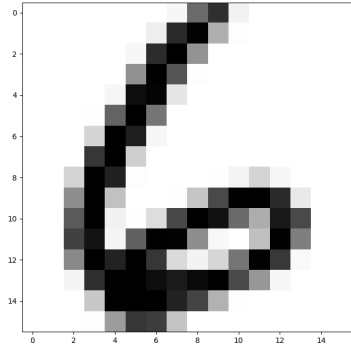
The main benefit of a full run of Algorithm 3 is the recovery of the combination of sparsity and non-mass splitting transport. For fast computations, we recommend performing just a single iteration of Algorithm 3, i.e., a single run of Algorithms 1 and 2.



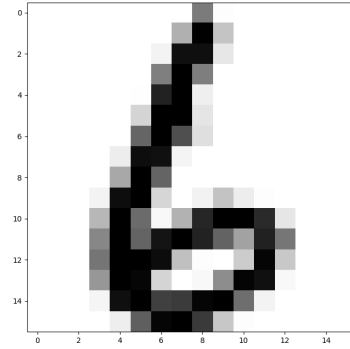
(5.1) Measure P_1



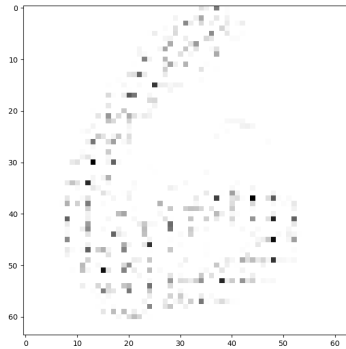
(5.2) Measure P_2



(5.3) Measure P_3

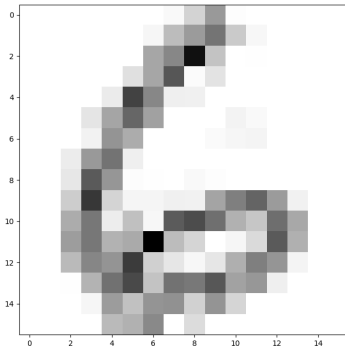


(5.4) Measure P_4

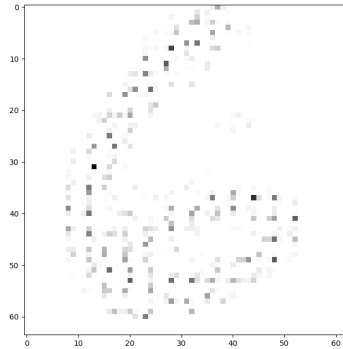


(5.5) Barycenter \bar{P}

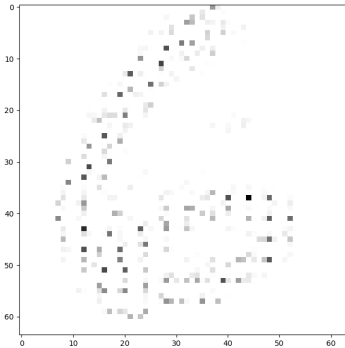
Fig. 5: Four measures P_1, \dots, P_4 , scans of handwritten digits six, supported on a 16×16 grid. The barycenter \bar{P} at the bottom.



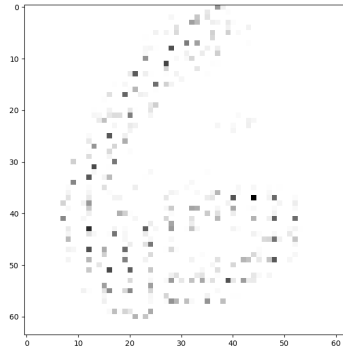
(6.1) Iteration 1, Step 1, Error 14.2%



(6.2) Iteration 1, Step 2, Error 4.3%



(6.3) Iteration 2, Step 1, Error 2.0%



(6.4) Iteration 2, Step 2, termination

Fig. 6: A sample run of Algorithm 3 for the measures in Figure 5. It already terminates after 2 iterations.

5.2 Scaling of Algorithm 1 and runs for Algorithm 3

Finally, we study the scaling of Algorithm 1 and the practical running time of our algorithms. Algorithm 1 is the main pillar of the two viable approaches in this paper for practical computations: either a single run of Algorithm 1 and 2 or a full run of Algorithm 3, if the problem size allows it. It is the only LP without a warm start. Algorithm 1 is based on an LP formulation using S_{org} as the set of possible support points. Before we turn to more computations, let us take a closer look at the number of variables and constraints in this LP to set up proper expectations. Using $|P_{\text{sum}}| = \sum_{i=1}^N |P_i|$, this LP has

$$|S_{\text{org}}| + |S_{\text{org}}| \cdot |P_{\text{sum}}| \text{ variables} \quad \text{and} \quad N \cdot |S_{\text{org}}| + |P_{\text{sum}}| \text{ constraints.}$$

Note $N \cdot |S_{\text{org}}| \geq |P_{\text{sum}}|$, so the number of constraints scales linearly in N and $|S_{\text{org}}|$. Further, note that the number of constraints is always lower than the number of variables ($|P_{\text{sum}}| \geq N$), and typically dramatically so ($|P_{\text{sum}}| \gg N$). The dominating factor in the number of variables is $|S_{\text{org}}| \cdot |P_{\text{sum}}|$. If the supports of the P_i are disjoint, then $|S_{\text{org}}| = |P_{\text{sum}}|$ and $|S_{\text{org}}| \cdot |P_{\text{sum}}| = |S_{\text{org}}|^2 = |P_{\text{sum}}|^2$; a quadratic scaling.

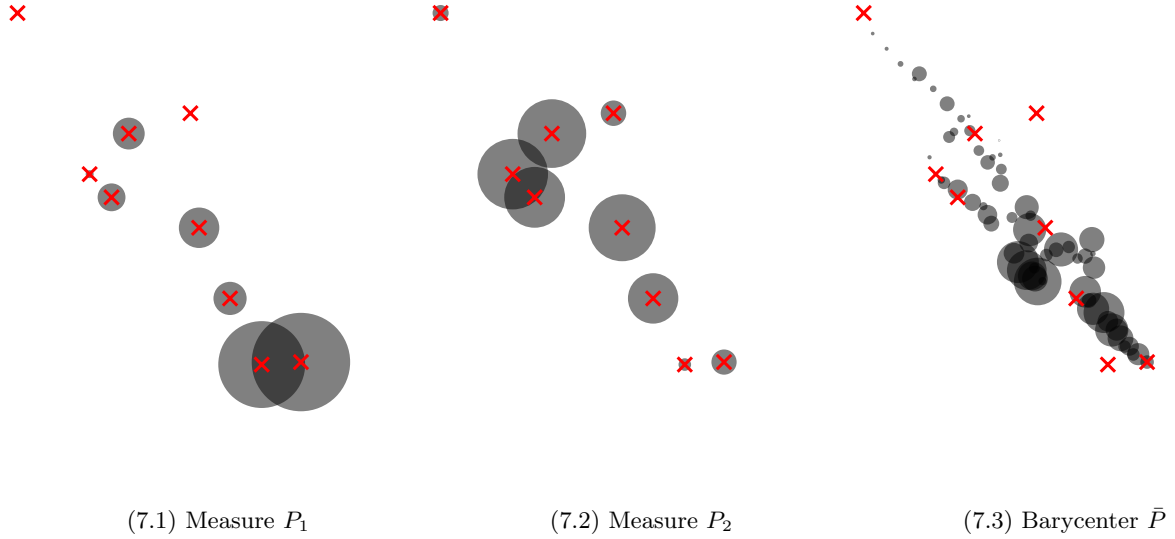


Fig. 7: Two (of eight) measures from a data set where the support points do not lie on a grid. All measures have the same support points with varying masses. The barycenter \bar{P} to the right.

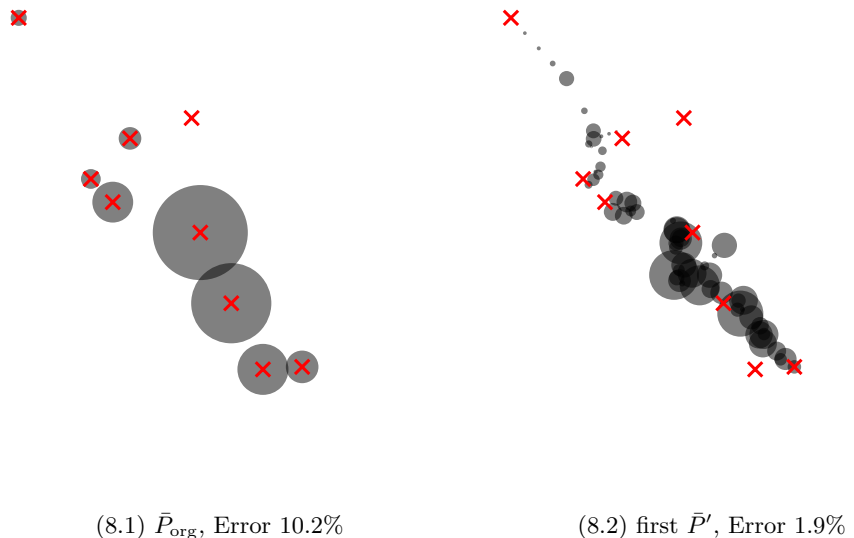


Fig. 8: Measures \bar{P}_{org} and \bar{P}' from the first iteration of Algorithm 3 for the data depicted in Figure 7. The algorithm terminates after the first iteration.

Two types of scaling are of interest: scaling the number N of measures and scaling $|S_{\text{org}}|$. For the sake of a simple analysis, we assume all measures have the same number of support points $|P_{\text{max}}|$. Then $|P_{\text{sum}}| = N \cdot |P_{\text{max}}|$.

Scaling for grid-structured data First, we consider scaling for grid-structured data. Let K denote the number of grid points in each direction. For 2-d data, the grid has K^2 points, which is an upper bound on $|P_{\text{max}}|$ and on $|S_{\text{org}}|$. Thus the number of variables is bounded by $K^2 + K^2 \cdot (N \cdot K^2)$ and the number of constraints is bounded by $N \cdot K^2 + N \cdot K^2 = 2(N \cdot K^2)$. Note that the bound on the number of variables is roughly $K^4 \cdot N$.

While the actual sizes of $|P_{\text{max}}|$ and $|S_{\text{org}}|$ are usually significantly smaller than K^2 , they typically remain a linear fraction of K^2 (for MNIST digits between $\frac{1}{5}$ and $\frac{1}{3}$), and so these bounds immediately imply two types of consequences: First, the scaling with the number N of measures is linear and we expect it to remain favorable. Second, doubling the density K of the underlying grids will multiply the number of variables by 16.

Let us turn to some computations. In Table 1, we report on average errors and completion times for a large number of runs of Algorithm 3. For each of these runs, we used random samples of 16×16 digits as the measures. Each row is based on the data from a total of 100 runs, 10 for each digit $0, 1, \dots, 9$. The table lists the initial error and time for the computation of an approximate barycenter \bar{P}_{org} in S_{org} (Algorithm 1), the error for the first \bar{P}' (Algorithm 2), the error, time, and number of iterations for a full run of Algorithm 3, and the time for an exact barycenter computation.

The first row shows numbers on random samples of four measures, as in the example depicted in Figures 5 and 6. We observed a termination of Algorithm 3 after an average of 2.2 iterations. This low number of iterations is not surprising, because of the low initial error and the implementation of Step 3 of Algorithm 2 (see above). Without this tweak to Step 3, the average number of iterations was 3.1 for four measures. The same effects extend to larger computations, where the approximation error of the initial \bar{P}_{org} is already low (much lower than the guaranteed bound of 2), most of the further improvement already happens towards the first \bar{P}' , and less than 4 iterations were necessary on average. The times include setup of the problems. We did not observe a clear pattern with respect to the errors for the first \bar{P}_{org} and \bar{P}' or the final approximation, but the average number of iterations of Algorithm 3 increases slightly for more measures.

We have been able to run Algorithm 3 for up to 20 measures in less than three minutes. In contrast, we have not been able to perform the computation of an exact barycenter for more than 8 measures, even using some refinements to the exact barycenter computation [10]. For larger number of measures, the difference between the running times becomes dramatic, even though grid-structured data, in fact, is a scenario where the exact LP does not scale exponentially (recall an exact barycenter is contained in an N -times finer grid) [10].

In contrast, computations in denser grids quickly become impossible due to the quadratic scaling of the underlying LP with respect to $|S_{\text{org}}|$. Recall that doubling the density K of a grid multiplies the number of variables by 16. Figure 9 shows the results of Algorithm 1 for 4 measures in a 32×32 grid and a 64×64 grid. The computations took about 5 minutes, respectively 92 minutes. The 64×64 example exceeds 10 million variables and is only solvable because of the extremely low number of constraints.

One has to be very careful when comparing these computational speeds to reported computations for other, non-LP based algorithms in the literature. It would be misleading to only observe that, for grid-structured problems, the scaling for increasingly dense grids is worse than for some popular algorithms [9,18,19,38] – for example, iterative Bregman

no. of measures	first \bar{P}_{org}		first \bar{P}'		full run of Alg. 3		exact
	error	time (s)	error	error	time (s)	iterations	time (s)
4	14.8%	4.2	3.8%	3.1%	9.9	2.2	120
5	15.2%	5.7	4.4%	4.1%	16.4	2.8	204
6	15.5%	8.5	4.5%	3.9%	22.3	2.7	540
7	15.1%	12.1	4.6%	4.2%	29.8	3.1	1602
8	16.2%	16.3	5.2%	4.8%	36.7	3.1	4330
9	?	23.0	?	?	45.2	3.4	—
12	?	39.1	?	?	74.8	3.3	—
16	?	58.4	?	?	99.3	3.7	—
20	?	90.3	?	?	169.2	4.5	—

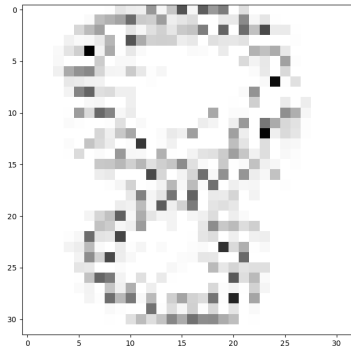
Table 1: Average numbers (error, time) for an initial approximation \bar{P}_{org} , first \bar{P}' , full runs of Algorithm 3, and an exact computation in a grid setting. The numbers in each row were derived from 100 random samples of 16×16 digits from the MNIST data set.

projection methods allowed us to run a test for 10 measures in a 28×28 grid (and approximate barycenter on the same grid S_{org}) in less than 30 seconds; for Radon and Sliced barycenters, there are reports on successful computations for three measures in 1024×1024 grids. We would like to stress that the problem variants tackled by these algorithms are very different (in both input and desired output) and much simpler – the goal of regularization and other simplifications to the objective function, as well as the search for dense solutions, is precisely to facilitate large-scale computations. The additional computational cost in our approach leads to a couple of favorable properties of the output: The guarantee of a 2-approximation, low practical error, sparsity, non-mass split, numerical stability, and support in S and not only in S_{org} . Our algorithm runs without specification of a fixed support set for the solution, and thus has the ability to work for any data.

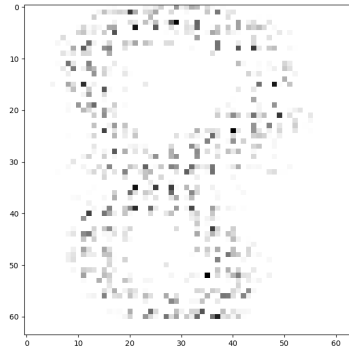
Additionally, we would like to note that grid data is arguably the *least* competitive setting for our algorithms in view of computational speed. Next, we turn to a best-case type of data for our algorithms.

Scaling for data in general position In contrast, applications in operations research and optimization often are based on a small set of geographical locations that do not exhibit an obvious structure. In this section, we consider data sets as depicted in Figure 7 – a set of N measures that all have the same support of size $|P_{\text{max}}|$. This configuration leads to a best-case scenario in that $|S_{\text{org}}| = |P_{\text{max}}|$, i.e., the union of original supports is the same as any of the supports. This has an extremely positive effect on the size of the LPs for Algorithm 1: The number of variables is $|P_{\text{max}}| + N \cdot |P_{\text{max}}|^2$ and the number of constraints is $2(N \cdot |P_{\text{max}}|)$. This contrasts with the (always) exponentially-sized set S , and corresponding LPs, for an exact computation of a barycenter for data in general position.

In Table 2, we report on average errors and completion times for runs of Algorithm 3. The numbers in each row were derived from 100 runs for the given number of measures of 9 random support points. The measures were constructed through a random assignment of varying masses to a fixed set of support points in general position. We also chose the weights λ_i randomly. The combination of data in general position, which makes a discretization of the underlying space unavailable, and a non-uniform weight vector makes for an impractical



(9.1) \bar{P}_{org} , 32×32 digits



(9.2) \bar{P}_{org} , 64×64 digits

Fig. 9: Approximate barycenters \bar{P}_{org} for a run of Algorithm 1 for 4 digits in 32×32 and 64×64 grids. These computations already took several minutes, respectively more than an hour. Computations in denser grids quickly become impossible due to the quadratic scaling of the underlying LP with respect to $|S_{\text{org}}|$.

no. of measures	first \bar{P}_{org}		first \bar{P}'		full run of Alg. 3		exact
	error	time (s)	error	error	time (s)	iterations	time (s)
8	10.1%	0.7	2.0%	1.6%	0.9	1.4	505
12	9.8%	1.1	2.4%	1.9%	3.0	1.8	12400
50	?	2.3	?	?	8.0	2.2	—
100	?	3.5	?	?	16.6	2.3	—
1000	?	18.5	?	—	—	—	—
10000	?	229.2	?	—	—	—	—

Table 2: Average numbers (error, time) for an initial approximation \bar{P}_{org} , first \bar{P}' , and full runs of Algorithm 3, and an exact computation for data in general position. The numbers in each row were derived from 100 runs on a set of measures with 9 support points of randomly chosen masses.

setting for most algorithms in the literature; see Section 1.1. This is why our comparisons are restricted to an exact, LP-based solution.

Exact computations in this setting are hard and thus approximation errors are not available for more than 12 measures of 9 support points. At the same time, the LP for Algorithm 1 for such an instance still is of trivial size: it has $12 \cdot 9^2$ variables and $2(12 \cdot 9)$ constraints. The speed-up over an exact computation for a set of 8 measures (the example in Section 5.2) is a factor of more than 600. This factor escalates quickly - for 12 measures our algorithm is already faster by a factor of more than 4000. Figure 10 shows some barycenters computed in this setting. All of the depicted examples were solved in a few seconds.

We have been able to run Algorithm 1 for more than 10000 measures in less than four minutes. Instances up to 1000 measures solve in less than 20 seconds. One of the main reasons for these low running times is the extremely low number of constraints. The same scalability of Algorithm 3 is not possible, as the size $|\bar{P}'|$ increases to a point where the LP

for the second iteration cannot be constructed anymore. (For 1000 measures, it would have close to 100 million variables.) It is important to note that the advantage of having the *same* support points in all measures implies an incredibly small S_{org} (and thus fast Algorithm 1), but the same does not hold for later iterations of Algorithm 3.

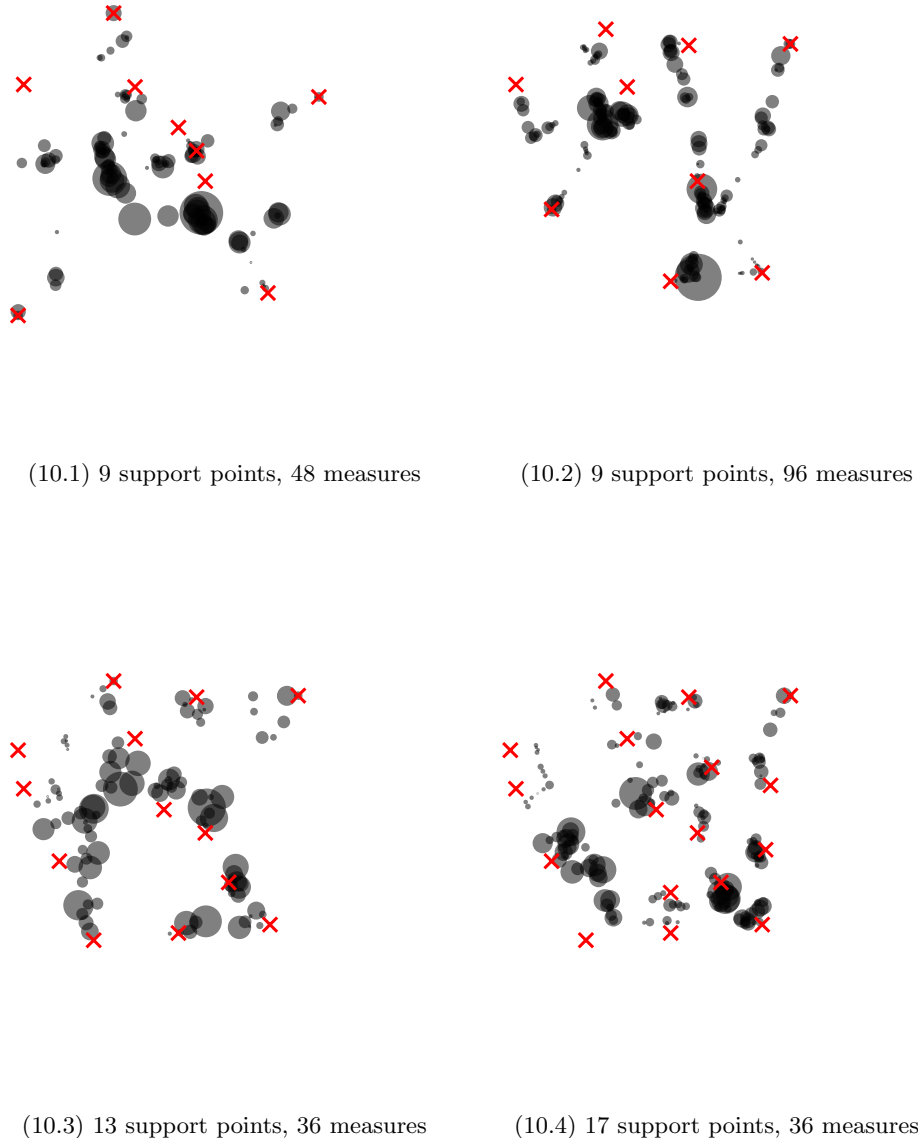


Fig. 10: Approximate barycenters \bar{P}' at the end of the first iteration of Algorithm 3 for different supports and numbers of measures. All of these computations completed in a matter of seconds.

The times reported in Table 1 include the setup of the problems. Again, we observe that \bar{P}_{org} is significantly improved in the first step towards \bar{P}' , and that further iterations do not change it noticeably anymore. The average number of iterations increases slowly with the number of measures. The increase is slower than in the grid-structured setting due to the general position of data – less repetition in the weighted centroids for different combinations means that later iterations of Algorithm 3 are less likely to further improve the solution.

Recall that the number of variables for Algorithm 1 is quadratic in the number of support points for each measure. Doubling the number of support points (which we basically do in one of the examples in Figure 10) increases the number of variables in the number of the problem by factor 4, the same effect as increasing the number of measures by factor 4. An instance with 2500 measures of 18 support points exhibits a similar running time for Algorithm 1 to the instance in the final row of Table 2.

Summing up, the combination of few, overlapping support points in a large number of measures is a best-case scenario for the combination of a single run of Algorithms 1 and 2. Applications in operations research, such as facility location problems, often fall precisely into this category. Their data is in general position, which does not pose an additional challenge for Algorithms 1 or 2. In contrast, this setting makes an exact computation impossible for any reasonable problem size and many algorithms in the literature are not designed to work (or work well) for such data. This is a setting in which we recommend use of the presented methods, in particular if interested in the favorable properties of its output.

Acknowledgments

The author would like to thank Ethan Anderes for the support with implementations in the Julia language, and Jacob Miller for the helpful discussions. The author gratefully acknowledges support through the Collaboration Grant for Mathematicians *Polyhedral Theory in Data Analytics* of the Simons Foundation.

References

1. M. Aguech and G. Carlier. Barycenters in the Wasserstein space. *SIAM Journal on Mathematical Analysis*, 43 (2):904–924, 2011.
2. E. Anderes, S. Borgwardt, and J. Miller. Discrete Wasserstein Barycenters: Optimal Transport for Discrete Data. *Mathematical Methods of Operations Research*, 84 (2):389–409, 2016.
3. G. Auricchio, F. Bassetti, S. Gualandi, and S. Veneroni. Computing Wasserstein Barycenters via Linear Programming. In *Integration of Constraint Programming, Artificial Intelligence, and Operations Research*, pages 355–363, 2019.
4. M. Beiglböck, P. Henry-Labordere, and F. Penkner. Model-independent bounds for option prices – a mass transport approach. *Finance and Stochastics*, 17 (3):477–501, 2013.
5. J.-D. Benamou, G. Carlier, M. Cuturi, L. Nenna, and G. Peyré. Iterative Bregman Projections for Regularized Transportation Problems. *SIAM Journal on Scientific Computing*, 37(2):A1111–A1138, 2015.
6. J. Bezanson, A. Edelman, S. Karpinski, and V. B. Shah. Julia: A fresh approach to numerical computing. *SIAM Review*, 59(11):65–98, 2017.
7. J. Bigot and T. Klein. Characterization of barycenters in the Wasserstein space by averaging optimal transport maps. *ESAIM: Probability and Statistics*, 22:35–57, 2017.
8. E. Boissard, T. Le Gouic, and J.-M. Loubes. Distribution’s template estimate with Wasserstein metrics. *Bernoulli*, 21 (2):740–759, 2015.
9. N. Bonneel, J. Rabin, G. Peyré, and H. Pfister. Sliced and Radon Wasserstein Barycenters of Measures. *Journal of Mathematical Imaging and Vision*, 51(1):22–45, 2015.
10. S. Borgwardt and S. Patterson. Improved Linear Programs for Discrete Barycenters. *INFORMS Journal on Optimization*, in print, available on arxiv:1803.11313, 2019.

11. G. Buttazzo, L. De Pascale, and P. Gori-Giorgi. Optimal-transport formulation of electronic density-functional theory. *Physical Review A*, 85:062502, 2012.
12. G. Carlier, V. Duval, G. Peyré, and B. Schmitzer. Convergence of Entropic Schemes for Optimal Transport and Gradient Flows. *SIAM Journal on Mathematical Analysis*, 49(2):1385–1418, 2017.
13. G. Carlier and I. Ekeland. Matching for teams. *Economic Theory*, 42 (2):397–418, 2010.
14. G. Carlier, A. Oberman, and E. Oudet. Numerical methods for matching for teams and Wasserstein barycenters. *ESAIM: Mathematical Modelling and Numerical Analysis*, 49 (6):1621–1642, 2015.
15. P-A. Chiappori, R. McCann, and L. Nesheim. Hedonic price equilibria, stable matching and optimal transport; equivalence, topology and uniqueness. *Economic Theory*, 42 (2):317–354, 2010.
16. S. Claici, E. Chien, and J. Solomon. Stochastic Wasserstein Barycenters. *Proceedings of the 35th International Conference on Machine Learning, PMLR* 80:999–1008, 2018.
17. C. Cotar, G. Friesecke, and C. Klüppelberg. Density functional theory and optimal transportation with Coulomb cost. *Communications on Pure and Applied Mathematics*, 66 (4):548–599, 2013.
18. M. Cuturi. Sinkhorn Distances: Lightspeed Computation of Optimal Transport. In *Advances in Neural Information Processing Systems*, volume 26, pages 2292–2300. 2013.
19. M. Cuturi and A. Doucet. Fast Computation of Wasserstein Barycenters. In *Proceedings of the 31st International Conference on Machine Learning (ICML-14)*, pages 685–693, 2014.
20. E. del Barrio, J.A. Cuesta-Albertos, C. Matrán, and A. Mayo-Íscar. Robust clustering tools based on optimal transportation. *Statistics and Computing*, 29(1):139–160, 2019.
21. M. Essid and J. Solomon. Quadratically Regularized Optimal Transport on Graphs. *SIAM Journal on Scientific Computing*, 40:A1961–A1986, 2017.
22. C. Frogner, F. Mirzazadeh, and J. Solomon. Learning Embeddings into Entropic Wasserstein Spaces. *eprint arXiv:1905.03329*, 2019.
23. S. Gadat, I. Gavra, and L. Risser. How to Calculate the Barycenter of a Weighted Graph. *Mathematics of Operations Research*, doi:10.1287/moor.2017.0896, 2018.
24. A. Galichon, P. Henry-Labordere, and N. Touzi. A stochastic control approach to non-arbitrage bounds given marginals, with an application to lookback options. *Annals of Applied Probability*, 24 (1):312–336, 2014.
25. A. Jain, Y. Zhong, and M.-P. Dubuisson-Jolly. Deformable template models: A review. *Signal Processing*, 71 (2):109–129, 1998.
26. A. Kroshnin, D. Dvinskikh, P. Dvurechensky, A. Gasnikov, N. Tupitsa, and C. Uribe. On the Complexity of Approximating Wasserstein Barycenter. *eprint arXiv:1901.08686*, 2019.
27. Y. LeCun, L. Bottou, Y. Bengio, and P. Haffner. Gradient-based learning applied to document recognition. *Proceedings of the IEEE*, 86(11):2278–2324, 1998.
28. S. P. Lloyd. Least squares quantization in pcm. *IEEE Transactions on Information Theory*, 28(2):129–137, 1982.
29. M. Lubin and I. Dunning. Computing in Operations Research Using Julia. *INFORMS Journal on Computing*, 27(2):238–248, 2015.
30. G. Luise, A. Rudi, M. Pontil, and C. Ciliberto. Differential Properties of Sinkhorn Approximation for Learning with Wasserstein Distance. *Advances in Neural Information Processing Systems (NIPS) 31*, pages 5859–5870, 2018.
31. G. Luise, S. Salzo, M. Pontil, and C. Ciliberto. Sinkhorn Barycenters with Free Support via Frank-Wolfe Algorithm. *eprint arXiv:1905.13194*, 2019.
32. J. B. MacQueen. Some methods of classification and analysis of multivariate observations. In *Proceedings of the Fifth Berkeley Symposium on Mathematical Statistics and Probability*, pages 281–297, 1967.
33. Y. Mileyko, S. Mukherjee, and J. Harer. Probability measures on the space of persistence diagrams. *Inverse Problems*, 27(12), 2011.
34. J. Miller. Transportation Networks and Matroids: Algorithms through Circuits and Polyhedrality, 2016. Ph.D. thesis, University of California Davis.
35. E. Munch, K. Turner, P. Bendich, S. Mukherjee, J. Mattingly, and J. Harer. Probabilistic Frechet means for time varying persistence diagrams. *Electronic Journal of Statistics*, 9:1173–1204, 2015.
36. Victor M. Panaretos and Yoav Zemel. Statistical Aspects of Wasserstein Distances. *Annual Review of Statistics and Its Application*, 6(1):405–431, 2019.
37. B. Pass. Multi-marginal optimal transport and multi-agent matching problems: Uniqueness and structure of solutions. *Discrete and Continuous Dynamical Systems A*, 34 (4):1623–1639, 2014.
38. G. Peyré and M. Cuturi. Computational optimal transport. *Foundations and Trends in Machine Learning*, 11(5-6):355–607, 2019.
39. J. Rabin, G. Peyré, J. Delon, and M. Bernot. Wasserstein Barycenter and its Application to Texture Mixing. *Scale Space and Variational Methods in Computer Vision. Lecture Notes in Computer Science*, 6667:435–446, 2012.

40. J. Solomon, F. de Goes, G. Peyré, M. Cuturi, A. Butscher, A. Nguyen, T. Du, and L. Guibas. Convolutional Wasserstein Distances: Efficient Optimal Transportation on Geometric Domains. *ACM Transactions on Graphics*, 34(4):66:1–66:11, 2015.
41. J. Solomon, R. Rustamov, L. Guibas, and A. Butscher. Earth Mover’s Distances on Discrete Surfaces. *ACM Transactions on Graphics*, 33(4):67:1–67:12, 2014.
42. S. Srivastava, C. Li, and D. B. Dunson. Scalable Bayes via Barycenter in Wasserstein Space. *Journal of Machine Learning Research*, 19:1–35, 2018.
43. M. Staib, S. Claici, J. Solomon, and S. Jegelka. Parallel Streaming Wasserstein Barycenters. *Advances in Neural Information Processing Systems (NIPS) 30*, pages 2644–2655, 2017.
44. E. Tardos. A strongly polynomial algorithm to solve combinatorial linear programs. *Operations Research*, 34(2):250–256, 1986.
45. A. Trouvé and L. Younes. Local Geometry of Deformable Templates. *SIAM Journal on Mathematical Analysis*, 37 (1):17–59, 2005.
46. K. Turner, Y. Mileyko, S. Mukherjee, and J. Harer. Fréchet means for distributions of persistence diagrams. *Discrete and Computational Geometry*, 52(1):44–70, 2014.
47. C. Villani. *Topics in Optimal Transportation*. American Mathematical Society, 2003.
48. C. Villani. *Optimal transport: old and new*. Springer, 2009.
49. L. Yang, J. Li, D. Sun, and K.-C. Toh. A Fast Globally Linearly Convergent Algorithm for the Computation of Wasserstein Barycenters. *eprint arXiv:1809.04249*, 2019.
50. J. Ye, P. Wu, J. Z. Wang, and J. Li. Fast Discrete Distribution Clustering Using Wasserstein Barycenter With Sparse Support. *IEEE Transactions on Signal Processing*, 65(9):2317–2332, 2017.
51. Y. Zemel and V. Panaretos. Fréchet Means and Procrustes Analysis in Wasserstein Space. *Bernoulli*, 25(2):932–976, 2019.